Socioeconomic impacts from coastal flooding in the 21st century China's coastal zone: A coupling analysis between coastal flood risk and socioeconomic development

He Xu[1,2,3], Xiyong Hou[1*], Shunqi Pan[3], Michaela Bray[3], Chengxin Wang[4]

[1]Yantai Institute of Coastal Zone Research, Chinese Academy of Sciences, Yantai, Shandong, P.R. China

[2]University of Chinese Academy of Sciences, Beijing, P.R. China

[3]Hydro-environmental Research Centre, School of Engineering, Cardiff University, Cardiff, United Kingdom

[4]College of Geography and Environment, Shandong Normal University, Jinan, P.R. China

*** Correspondence:**

Xiyong Hou (xyhou@yic.ac.cn)

Keywords: coastal flooding, socioeconomic impact, coupling coordination degree, coastal flood risk, socioeconomic development level, China's coastal zone

Abstract:

Coastal flooding due to sea level rise significantly affects socioeconomic development. The dynamic nature of coastal flood risk (CFR) and socioeconomic development level (SDL) leads to uncertainties in understanding their future interplay. This ambiguity challenges coastal nations in devising effective flood adaptation and coastal management strategies. This study quantitatively examines the expected GDP affected (EGA) and population affected (EPA) by coastal flooding in China's coastal zone (CCZ) from 2030 to 2100 under various climate scenarios (RCP2.6-SSP1, RCP4.5-SSP2, and RCP8.5-SSP5). The future SDL in CCZ is assessed using a method combining the analytic hierarchy process with entropy weight. The future CFR-SDL dynamic relationship is analyzed using the coupling coordination degree (CCD) model. The results reveal that in CCZ under the RCP2.6-SSP1, RCP4.5-SSP2, and RCP8.5-SSP5 scenarios: by 2100, the EGA and EPA will reach \$814.90 billion & 6.17 million people, \$828.16 billion & 7.63 million people, and \$1568.83 billion & 8.05 million people, respectively, where the coastal cities in Jiangsu and Guangdong provinces will face more obvious risks of socioeconomic losses; The total area in the CCZ at "Very high" and "High" level of socioeconomic development by 2100 is projected to reach 11.33×10^3 km^2, 12.86×10^3 km^2, and 15.82×10^3 km^2, respectively, with the Pearl River Delta, Yangtze River Delta, and Tianjin-Hebei remaining pivotal for CCZ's socioeconomic growth. Cities such as Lianyungang, Jiaxing, Shenzhen, Dongguan, and Foshan show notable CCD characteristics, and addressing the trade-off between SDL

and CFR is crucial in achieving sustainable development. This study highlights the potential socioeconomic impacts of coastal flooding and emphasizes the importance of considering the interrelationship between CFR and SDL when developing coastal flood adaptation policies.

1. Introduction

Coastal flooding induced by sea level rise (SLR) due to global climate change is a serious environmental and socioeconomic problem, posing obvious risks to people's lives, economic development, and the ecological environment in coastal zones around the world (Nicholls and Cazenave, 2010; Vousdoukas et al., 2018; Edmonds et al., 2020; Nicholls et al., 2021). With superior natural and socioeconomic conditions, there are currently over 898 million people living in low-lying coastal areas worldwide, generating over $12.57 trillion in Gross Domestic Product (GDP) (Kirezci et al., 2023). By 2050, the population and GDP in the coastal zones are expected to exceed 839 million and $17.54 trillion, respectively (Merkens et al., 2016; Kirezci et al., 2023). However, according to the assessment reports of the Intergovernmental Panel on Climate Change (IPCC) (IPCC, 2019, 2021), the global mean sea level will continue to rise in the future, leading to an increased impact on populations and economies of coastal areas (Hallegatte et al., 2013; Merkens et al., 2018). Recently, there has been seen a growing number of studies focusing on the risks associated with global SLR. For instance, Vousdoukas et al. (2018) found that without further investment in coastal adaptation, the annual economic losses due to extreme SLR in Europe are expected to be between 93 and 961 billion *euros* by the end of the century, with the number of people exposed to coastal flooding reaching 1.52~3.65 million annually. Moreover, Kirezci et al. (2023) reported that without effective adaptation to the extreme SLR, the number of people affected would reach 246 million by 2100, and expected annual damage would reach 2.9% of global GDP. Therefore, given the significance of the impacts of SLR due to the global climate change, it is vital to investigate as well as quantify the spatiotemporal variation characteristics of the expected GDP affected (EGA) and expected population affected (EPA) by the coastal flooding under different scenarios in the future period, in particular the combined coastal flood risk and impacts on socioeconomic development, so that adequate and effective coastal flood adaptation policies can be developed.

China has approximately 18,000 km mainland coastline from the Yellow Sea in the north to the Gulf of Tonkin in the south, along the intersection of the Eurasian continent and the Pacific Ocean. China's coastal zone (CCZ) covers part of 14 provinces and regions, namely Liaoning, Hebei, Tianjin, Shandong, Jiangsu, Shanghai, Zhejiang, Fujian, Guangdong, Hong Kong, Macau, Guangxi Hainan and Taiwan (Aitsi-Selmi et al., 2016; Du et al., 2022), with an area over 1.33 million km^2 which is closely adjacent to the coast as shown in Fig. 1. It is a key contributor to China's economic development, as megacities such as Shanghai, Guangzhou, Shenzhen, and Hong Kong are situated along the coast, accommodating more than 40% of the country's population and contributing over

60% of the country's GDP (Fang et al., 2020). According to the 2022 China Statistical Yearbook, the population and GDP of China's coastal provinces reached 636.82 million people and 60,425.74 billion CNY (RMB *yuan)* in 2021. Additionally, CCZ also encompasses a wide range of ecosystems, including sandy beaches, rocky shores, estuaries, mangroves, and coral reefs, etc. (Liu et al., 2021).

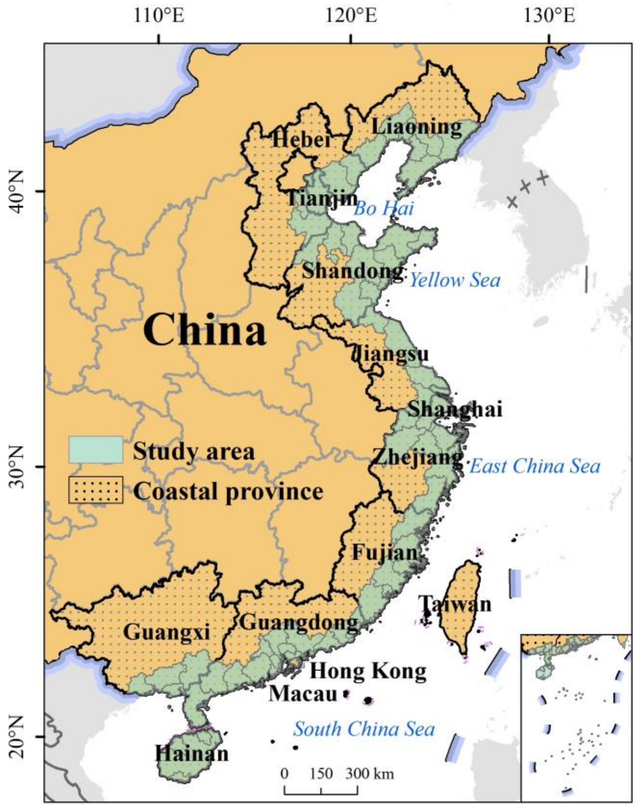

Fig. 1. Location of the China's coastal zone.

CCZ holds particular significance as one of the world's most densely populated and rapidly developing areas, with a concentration of economic activities and critical infrastructure along the coast (Du et al., 2022). Nevertheless, the population and GDP in this area are also highly exposed to coastal flooding due to the modest elevation above sea level, extreme weather events, dense river network, and higher than the global average rate of SLR (Wang et al., 2017; Xu et al., 2022a; Ministry of Natural Resources of the P. R. China, 2023). While numerous prior studies have examined the expected socioeconomic impacts of coastal flooding at a regional scale, such as in Shanghai (Yan et al., 2016; Chen et al., 2018), Xiamen (Xu et al., 2016), and the Pearl River Delta (Yang et al., 2015), only limited studies have been undertaken at the macroscopic scale of the CCZ (Cui et al., 2018; Fang et al., 2020). However, these large-scale studies solely quantified the socioeconomic losses in coastal provinces, while neglecting the losses in individual coastal cities. Such a limitation hampers the comprehension of spatial variations in socioeconomic losses and the development of suitable urban planning strategies by national policymakers.

Enhancing the resilience of coastal zones to coastal flooding requires a deeper understanding of the interactions between coastal flood risk (CFR) and socioeconomic development level (SDL). To date, several studies have investigated the CFR at different scales of the CCZ (Fang et al., 2016; Liao et al., 2019; Fang et al., 2020; Gao et al., 2020; Shi et al., 2020; Xu et al., 2022a). Although these studies included some socioeconomic indicators in the CFR assessment, the change in characteristics of SDL and the interrelationship between CFR and SDL in the CCZ in the future are not yet clear. The analytic hierarchy process (AHP) - entropy weight (EW) combined method (AHP-EW) provides a powerful tool for determining the weights of SDL assessment indicators based on projection data in the future. This method combines the subjective weight calculated by AHP based on the subjective judgment of experts and the objective weight calculated by EW based on the information entropy content of the data to obtain the final weight, which is more scientific and has been widely used in economic development and risk assessment research (Wu et al., 2017; Xiao et al., 2022). The coupling coordination degree model (CCDM), originally derived from physical sciences, plays an important role in assessing the interrelationship between two or multiple systems (Liu et al., 2021). Conceptually, the CCDM posits that a higher degree of coupling coordination symbolizes a more intertwined relationship between systems, while a lower degree implies a weaker or more independent connection. This model has been widely applied in recent years, particularly in evaluating the nexus between socioeconomic development and disaster risk. For instance, Li et al. (2021) devised the CCDM to investigate the interplay between urbanization and natural disasters in the Pearl River Delta. Liu et al. (2022) developed an improved CCDM to analyze the coupling coordination in urbanization-flood disaster systems in China. Hu et al. (2022) employed the CCDM to evaluate the coupled relationship between flood risk and socioeconomic development in the Yellow River Basin, China. Liu et al. (2023) adopted the coupling harmonious degree model to measure and calculate the interval index differences in the marine economic quality and urban resilience level of major coastal cities in China. Despite these developments, the exploration of the relationship between CFR and SDL in CCZ remains inadequately addressed, particularly under the ongoing challenges of rising sea levels, changing population size, and rapid economic growth. Revealing the coupling coordination relationship between SDL and CFR is crucial at a macro-scale. Such insights can significantly aid policymakers in optimizing resource allocation and setting strategic priorities, especially in regions where striking a balance between economic advancement and disaster risk minimizing is imperative. Additionally, scenario analysis is extensively employed by the IPCC, serving as a crucial tool for assessing the interactions between the human-environmental system and projecting future trends. After nearly a decade of development, numerous communities have collaboratively constructed scenario analysis frameworks, exemplified by the Representative Concentration Pathway (RCP) and the Shared Socio-economic Development Pathway (SSP), in order to enhance comprehension of the potential consequences of various decisions on climate change, sea-level rise (SLR), and socioeconomic development.

To this end, it is imperative to further quantify the coupling coordination degree between CFR and SDL after assessing the socioeconomic impacts of coastal flooding in the CCZ under different scenarios in the future. Such a quantification will aid policymakers and stakeholders in comprehending the potential impacts of coastal flooding on the regional economy, infrastructure, and human well-being. Therefore, this study aims to achieve the following objectives: (i) Analyze and quantify the changing spatiotemporal dynamics of the EGA and EPA resulting from coastal flooding in CCZ from 2030 to 2100 under the RCP2.6-SSP1, RCP4.5-SSP2, and RCP8.5-SSP5 scenarios, utilizing the depth-affected function; (ii) Investigate the spatiotemporal variation of the SDL and its changing characteristics in CCZ from 2030 to 2100 under different scenarios using the AHP-EW combined method; and (iii) Analyze the spatiotemporal variation of the CCD between CFR and SDL in CCZ from 2030 to 2100 under different scenarios using the CCDM. Furthermore, the findings of this study will yield valuable insights into the effectiveness of current adaptation measures and inform the development of future strategies to mitigate the impacts of coastal flooding, ultimately contributing to the achievement of sustainable development goals (SDGs) set by the United Nations, such as SDG 11 and 14.

The remainder of this paper is organized as follows. Section 2 describes the geography of the study area, datasets, and methods. Section 3 shows the results of the expected GDP/population affected due to coastal flooding, the future socioeconomic development level assessment, and the interaction between CFR and SDL. Section 4 discusses the findings, limitations, and future work. Finally, the conclusions are given in Section 5.

2. Material and methods

2.1 Study area

In this paper, the study area is focused on the administrative divisions of prefecture-level cities along the eastern coast of mainland China, as illustrated in Fig. 1, but excluding Hong Kong, Macao, Taiwan, and the islands in the South China Sea due to the unavailability of demographic and economic data. Additionally, considering the administrative jurisdictional relations, Hainan Island (province) is separated into three district-level cities (Haikou, Sanya, Danzhou) and other cities. Thus, the study area consists of a total of 11 coastal provinces (autonomous regions and municipalities) with a total of 63 coastal cities. Details of each coastal city, including its ID number, area, and province, are presented in Table S1.

2.2 Datasets

The datasets used in this study for analysis include the inundation data adopted from a numerical model, coastal risk data and socioeconomic projection data as detailed below.

2.2.1 Inundation depth data

The inundation depth data were obtained from the coastal flood inundation dataset, which was calculated in the previous study (Xu et al., 2022b) with a spatial resolution of 100 m. Within the inundation extent calculated by the hydraulic connectivity model (HCM), inundation depth was calculated by deducting the terrain elevation from the water level value simulated by the finite volume coastal and ocean model (FVCOM) from 2021 to 2100 under the RCP2.6, 4.5, and 8.5 scenarios. To match the spatial resolution of the socioeconomic data, the inundation depth data were upscaled to 1 km using the mean value method.

2.2.2 Coastal flood risk data

The coastal flood risk data were calculated by an assessment framework of coastal flood risk in the CCZ in the previous study (Xu et al., 2022a). The assessment framework encompasses three dimensions of hazard, exposure & sensitivity, and adaptive capacity considering 22 indicators for 2030, 2050, and 2100 under the combined scenarios of RCP2.6-SSP1, RCP4.5-SSP2, and RCP8.5-SSP5. While the original data resolution was 100 m, we resampled it to 1 km in this study to align with the socioeconomic data.

2.2.3 Socioeconomic projection data

The socioeconomic projection data for GDP, population, and land use/land cover (LULC) in the future period were obtained from Wang and Sun (2022), Chen et al. (2020), and Song (2021), respectively. All data selected are of high resolution and quality in known studies to date.

The GDP projection data were estimated for the period 2030-2100 at 10-year intervals for all five Shared Socioeconomic Pathways (SSP1-5) in 2005 Purchasing Power Parity (PPP) USD, with a spatial resolution of 30 arc seconds (~1 km). This dataset provides higher resolution data than several commonly used GDP projection datasets, including Gaffin et al. (2004), Murakami et al. (2021), and Jiang et al. (2022).

The population projection data were calculated by age, sex, and education level for each province of China for the period 2010-2100 under various SSP scenarios and downscaled to a spatial resolution of 30 arc seconds (~1 km) using the Representative Concentration Pathway (RCP) urban grid and historical population grid as a reference.

The LULC projection data were simulated using the System Dynamics-Future Land Use Simulation (SD-FLUS) model for the period from 2021 to 2100 under the RCP2.6-SSP1, RCP4.5-SSP2, and RCP8.5-SSP5 combined scenarios, with a spatial resolution of 100 m. To characterize the socioeconomic attributes, in this study, the gridded LULC data is upscaled to a 1 km resolution, indicating the area proportion of built-up area for each grid.

2.3 Methods

2.3.1 Methodology framework

The assessment of the socioeconomic impact of coastal flooding in the CCZ seeks to address the following research questions: (i) What will be the spatiotemporal characteristics of the EGA and EPA caused by coastal flooding in future periods? (ii) What are the dynamic characteristics of SDL in the future in CCZ? (iii) What are the spatiotemporal characteristics of the CCD between CFR and SDL in the future period? To enhance our interpretation of the methods for socioeconomic impact assessment of coastal flooding in the CCZ, we developed an illustrative framework comprising three modules (Fig. 2):

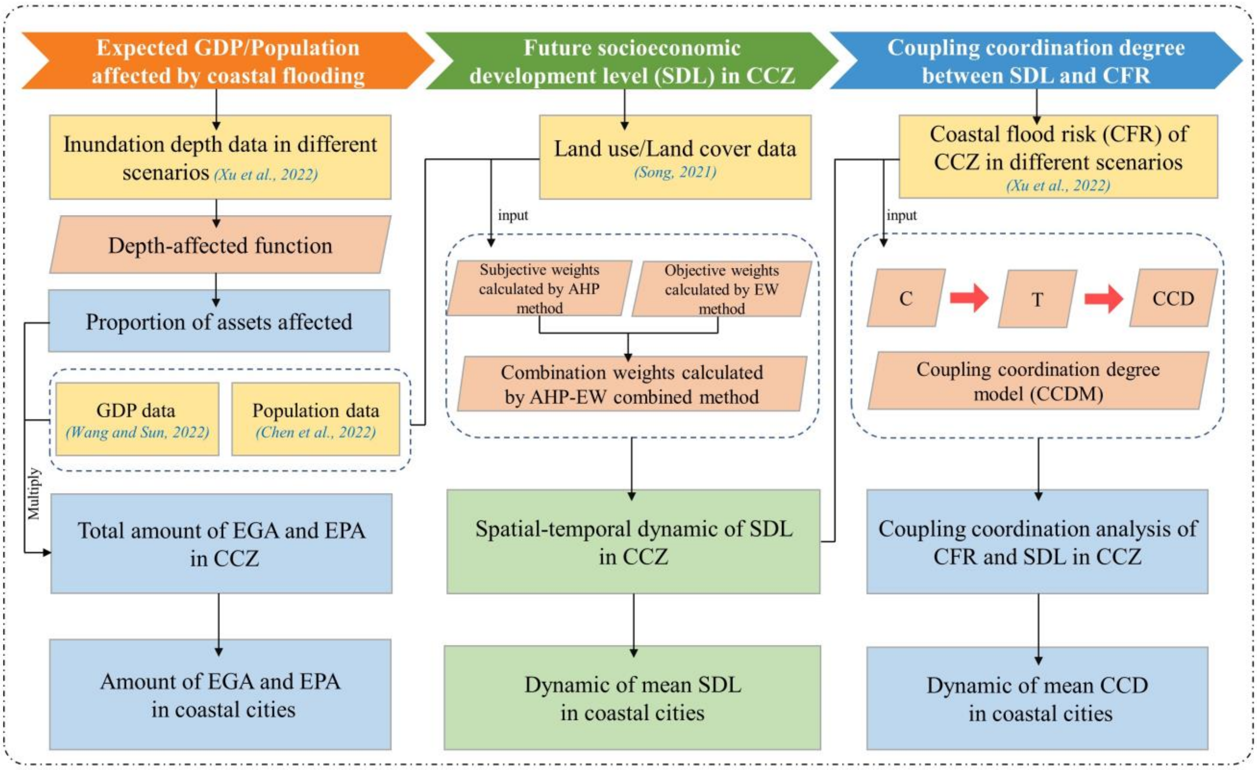

Fig. 2. The assessment framework of the socioeconomic impact of coastal flooding in the CCZ.

2.3.2 Selection of scenarios

Scenarios are descriptors that assess the likelihood of future development changes. They follow the principles of coherence and entail assumptions about critical drivers and relationships (Ramirez et al., 2015). To assess the socioeconomic impacts of coastal flooding under different future scenarios, internationally recognized Representative Concentration Pathways (RCPs) (van Vuuren et al., 2011) and Shared Socioeconomic Pathways (SSPs) (O'Neill et al., 2014) are utilized in this study. The RCPs and SSPs can be combined to form a two-dimensional RCP/SSP matrix (van Vuuren and Carter, 2014). This study specifically utilized three recommended scenarios: (i) RCP2.6-SSP1 scenario, envisioning a future with limited global warming, minimal environmental impact, and sustainable socio-economic development; (ii) RCP4.5-SSP2 scenario, describing a future where moderate climate policies are implemented and implying a mix of renewable and fossil fuel-based energy sources, moderate socioeconomic development, and efforts to balance environmental concerns with economic growth; and (iii) RCP8.5-SSP5 scenario, portraying a future characterized by high emissions, rapid economic growth, and limited climate policy actions (Engström et al., 2016; Deng et al., 2021). In addition, the periods of 2030, 2050, and 2100 represent short-term, mid-term, and long-term time scales, respectively, following the developmental stages suggested by Tebaldi et al. (2012) and Spirandelli et al. (2016).

2.3.3 Quantification of expected GDP/population affected

The depth-affected function is a useful tool for estimating the expected impact caused by floods (Messner, 2007; Hinkel et al., 2014). It provides an effective way to estimate the percentage of asset value that will be affected based on the depth of flooding. The function typically takes the form of a declining curve, indicating that the additional impact decreases as the inundation depth increases. In this study, the proportion of assets affected (PAA) as suggested by Hinkel et al. (2014) and Kirezci et al. (2023) is adopted as:

$$PAA = \frac{d}{d+1} \tag{1}$$

where d is the inundation depth (m). The PAA is then divided into five levels, namely 0-20%, 20%-40%, 40%-60%, 60%-80%, and 80%-100% as "Very low", "Low", "Medium", "High", and "Very high" levels of impacts, respectively.

Based on the PAA, the effective number of expected GDP/population affected (EGA/EPA) can be estimated with the following:

$$EGA = \sum_{i=1}^{n} PAA_i \cdot NG_i \tag{2}$$

$$EPA = \sum_{i=1}^{n} PAA_i \cdot NP_i \tag{3}$$

where *i* represents the serial number of the grid, *n* is the number of inundated grids, PAA_i denotes the proportion of assets affected in the *i*-th grid, and NG_i and NP_i are the GDP and population numbers of the i-th grid, respectively.

2.3.4 Assessment of future socioeconomic development level

In this study, the AHP-EW combined method serves as a tool for assessing future SDL, as it blends subjective weights calculated by AHP and objective weights calculated by EW to increase the scientificity of the weight calculation (Liu et al., 2020; Xiao et al., 2022; Xu et al., 2022a). This assessment involves four steps, as illustrated below:

First, the assessment indicators are normalized. For example, the GDP, population, and LULC data of the socioeconomic projection data are normalized based on the following Eq. (4).

$$N = \frac{X - X_{min}}{X_{max} - X_{min}} \tag{4}$$

where *N* represents the normalized indicator value, *X* represents the grid value, and X_{min} and X_{max} are the minimum and maximum values, respectively, for each indicator.

Second, subjective weights are calculated by AHP. The AHP method enables the determination of evaluation indicator weights through expert experience and knowledge. For this study, the qualitative assessments of socioeconomic indicators are determined by five expert considerations in climate change response, climate resilience, vulnerability assessment of coastal zones, and integrated management of coastal zones. These expert considerations construct a comparison matrix for these indicators using 1–9 scales developed by Saaty (2008) (Table S2). To ensure the accuracy of expert evaluations in the pairwise comparison matrix, a consistency ratio (CR) is computed. A CR value below 0.1 is considered acceptable consistency, which is determined using Eq. (5) and Eq. (6).

$$CR = \frac{CI}{RI} \tag{5}$$

$$CI = \frac{\lambda_{max} - n}{n - 1} \tag{6}$$

where *CI, RI,* λ_{max}, and *n* represent the consistency index, random index, maximum eigenvalue, and matrix order, respectively.

In determining the qualitative assessments of socioeconomic indicators, the indicator weights (W_{AHP}) using a standard AHP linear scale are used in the integration of individual judgments, which are 0.5396, 0.2970 and 0.1634 for GDP, Population, and LULC, respectively, with a low *CR* (0.01).

Third, objective weights are derived from the information entropy content of the indicators (Table 1). Suppose there are *m* grids within the CCZ specified for EW calculation, each grid possesses n indicators represented as X_{ij} (where *i*=1,2,3...m, and *j* =1,2,3...n), which are normalized to N_{ij} according to Eq. (4). The feature weight (Q_{ij}) of the *i*-th grid concerning the *j*-th indicator is computed using Eq. (8), the entropy value (e_j) is deduced through Eq. (9), and the variability coefficient (g_j) is determined via Eq. (10). These derived parameters then inform the calculation of the assessment indicator weight (W_{EW}) using Eq. (7). The calculation formulas are as follows:

$$W_{EW_j} = \frac{g_j}{\sum_{j=1}^{n} g_j}, j = 1,2,3 \ldots n \tag{7}$$

where

$$Q_{ij} = \frac{N_{ij}}{\sum_{i=1}^{m} N_{ij}} \tag{8}$$

$$e_j = -\frac{1}{ln\, n}\sum_{i=1}^{m} Q_{ij}\, ln\left(Q_{ij}\right), 0 \le e_j \le 1 \tag{9}$$

$$g_j = 1 - e_j \tag{10}$$

Table 1 Values of indicator weight ($\boldsymbol{W_{EW}}$ *) by EW method*

Indicators	**RCP2.6-SSP1**			**RCP4.5-SSP2**			**RCP8.5-SSP5**		
	2030	**2050**	**2100**	**2030**	**2050**	**2100**	**2030**	**2050**	**2100**

GDP	0.4327	0.3805	0.3479	0.4472	0.4116	0.3757	0.4412	0.3892	0.3542
Population	0.3082	0.3747	0.4350	0.2968	0.3474	0.4045	0.2963	0.3634	0.4286
LULC	0.2591	0.2448	0.2172	0.2560	0.2410	0.2198	0.2625	0.2474	0.2173

Finally, the combined weights are determined utilizing the AHP-EW combined approach. In order to incorporate the experts' subjective judgments on SDL and the objective information entropy characteristics of indicators, a linear combination method is applied to ascertain the combination weights (W_z) for SDL evaluation. The calculation formula utilized is as:

$$W_z = \alpha \cdot W_{AHP} + \beta \cdot W_{EW} \tag{11}$$

where α and β indicate the respective weight coefficients of AHP and EW, which are calculated using the distance formula, as shown in follows (Liu et al., 2020):

$$d(W_{AHP}, W_{EW}) = \left[\frac{1}{2}\sum_{j=1}^{n}(W_{AHP} - W_{EW})^2\right]^{\frac{1}{2}} \tag{12}$$

$$D = |\alpha - \beta| \tag{13}$$

$$\begin{cases} d(W_{AHP}, W_{EW})^2 = (\alpha - \beta)^2 \\ \alpha + \beta = 1 \end{cases} \tag{14}$$

where $d(W_{AHP}, W_{EW})$ indicates the distance between W_{AHP} and W_{EW}, D is the distinction in distribution coefficients. The combined weights ($\boldsymbol{W_z}$) are list in Table 2.

Table 2 Values of the combined weight ($\boldsymbol{W_z}$) by AHP-EW method

Indicators	**RCP2.6-SSP1**			**RCP4.5-SSP2**			**RCP8.5-SSP5**		
	2030	**2050**	**2100**	**2030**	**2050**	**2100**	**2030**	**2050**	**2100**
GDP	0.4916	0.4710	0.4602	0.4977	0.4828	0.4695	0.4953	0.4742	0.4622
Population	0.3020	0.3305	0.3541	0.2969	0.3194	0.3430	0.2967	0.3259	0.3519
LULC	0.2064	0.1985	0.1857	0.2054	0.1979	0.1876	0.2081	0.1999	0.1859

In summary, the combination weights of each indicator in the SDL assessment are calculated using Eqs. (4~14). The SDL value is obtained by weighting and summing the normalized indicator values based on the combined weight values, as shown in Eq. (15).

$$SDL = \sum\nolimits_{i=1}^{n} W_{zi} \cdot N_i \tag{15}$$

where n is the total number of indicators, W_{zi} is the combination weight of the i-th indicator, and N_i denotes the normalized value of the i-th indicator.

In order to demonstrate the spatiotemporal variation patterns of SDL and compare the fluctuations in SDL values across different scenarios and years, the SDL values are classified into five levels: "Very low", "Low", "Medium", "High", and "Very high", corresponding to the intervals <0.2, 0.2-0.4, 0.4-0.6, 0.6-0.8, and >0.8, respectively. As per the criteria and meanings of SDL levels, this study collectively refers to the "High" and "Very high" levels of SDL as the "Typical" level. ArcGIS software is used for visualization. Moreover, for each year in each scenario, the mean value of SDL (MSDL) for each coastal city is calculated and presented after being divided into five levels using a Jenks natural break technique in ArcGIS.

2.3.5 Coupling coordination analysis between CFR and SDL

The coupling coordination degree (CCD) model is developed to evaluate the interaction and coordination between different systems, indicating whether they have a companion relationship. This model has been widely used to study the relationships between land use, flood disasters, ecosystem services, and the social economy (Sun et al., 2019; Gan et al., 2021; Hu et al., 2022). This approach aims to reveal the change characteristics of the coupled relationship between these two systems from the near-term to the long-term under different scenarios. In this study, the CCD between CFR and SDL in the CCZ is assessed by the following:

$$CCD = \sqrt{C \cdot T} \tag{16}$$

in which,

$$C = \sqrt{\frac{(D \cdot S)}{((D + S)/2)^2}} \tag{17}$$

$$T = \gamma \cdot D + \delta \cdot S \tag{18}$$

where C is the coupling degree, D is the CFR index, and S is the SDL index. T denotes the coordination degree between CFR and SDL, where γ and δ are the weights of CFR and SDL, respectively. In this study, the importance of CFR and SDL is assumed to be equal, hence $\gamma = \delta = 0.5$.

Similar to the evaluation of SDL, the CCD value is also divided into five levels according to Table 3. The “High” and “Very high” CCD levels are collectively referred to as the “Typical” level. Moreover, in order to show the dynamics of the mean CCD (MCCD) of coastal cities in the CCZ, the MCCD of each coastal city is calculated, divided into five levels based on the natural breaks (Jenks) technique and visualized using ArcGIS.

Table 3 Discriminating standard of CCD between CFR and SDL

CCD level	Range	Meaning
Very low	0.0 – 0.2	Seriously imbalanced development
Low	0.2 – 0.4	Moderately imbalanced development
Medium	0.4 – 0.6	Slightly imbalanced development
High	0.6 – 0.8	Moderate coordinated development
Very high	0.8 – 1.0	High coordinated development

3. Results

3.1 Expected GDP/population affected by coastal flooding

3.1.1 Proportion of assets affected (PAA)

Fig. 3 shows the spatiotemporal variations of the pre-defined PAA levels. In general, the PAA levels are similar in pattern across different future scenarios. Regions labeled as "High" level are primarily situated in the northern part of the Yellow River Delta region in the Shandong coastal zone, the central-eastern portion of the Jiangsu coastal zone, and the Pearl River Delta region within the Guangdong coastal zone. Although areas classified under the "Very High" level experience more pronounced impacts, they cover a relatively smaller spatial extent. These "Very high" zones are mainly concentrated in low-elevation coastal areas and estuaries of various coastal provinces, such as the Liaoning coastal zone, the northwest corner of the Shandong coastal zone, the eastern sector of the Jiangsu coastal zone, the estuary of the Yangtze River, and the northwest coast of Taiwan. In terms of the areas affected under different risk level, the side bars in Fig.3 show that by 2100, the "High" level encompasses the largest areas under all three scenarios, covering 19.43×10^3 km^2, 20.25×10^3 km^2, and 23.08×10^3 km^2 by 2100 respectively, while the "Low" level holds the smallest affected areas, covering 8.46×10^3 km^2, 8.54×10^3 km^2, and 8.69×10^3 km^2, respectively.

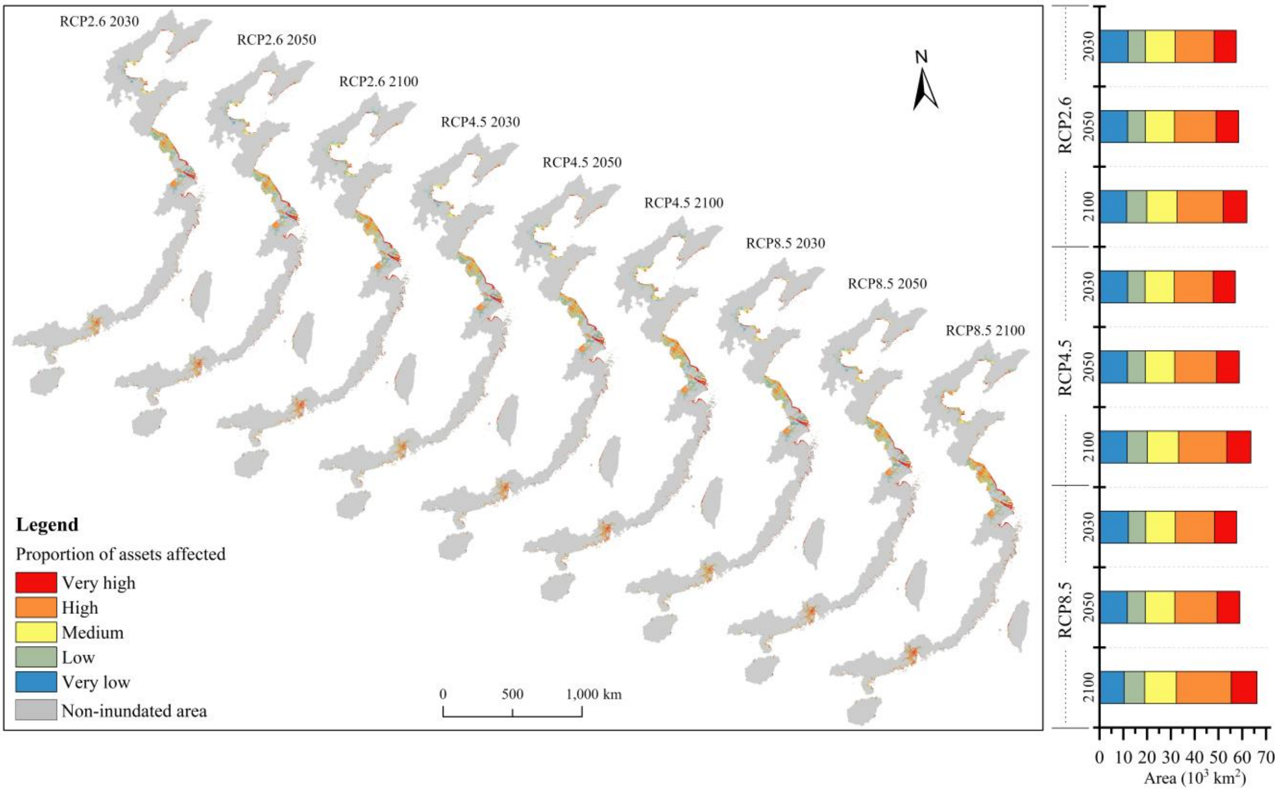

Fig. 3. Spatiotemporal distribution of PAA by 2030, 2050, and 2100 under RCP2.6, RCP4.5, and RCP8.5 (side bars showing the total area in CCZ affected under different PAA levels)

3.1.2 Expected GDP and population affected

Fig. 4a shows the values of EGA and EPA under the influence of coastal flooding exhibit a remarkable disparity between 2030 and 2100 in the CCZ. Specifically, under the RCP2.6-SSP1 scenario, the values of EGA show a sharp upswing, surging from \$460.65 billion by 2030 to \$848.17 billion by 2050 and then gradually decreasing to \$814.90 billion by 2100, resulting in a total increase of 76.90%. Meanwhile, the values of EPA diminish considerably from 10.30 million by 2030 to 6.17 million by 2100, decreased by 40.13%. Under the RCP4.5-SSP2 scenario, the value of EGA increases significantly from $401.87 billion by 2030 to $828.16 billion by 2100, with an impressive growth of 106.08%. Conversely, the number of EPA experiences a rapid descent from 10.55 million by 2030 to 7.63 million by 2100, reflecting a 27.68% decrease. Additionally, under the RCP8.5-SSP5 scenario, the EGA value surges from $512.11 billion by 2030 to $1568.83 billion by 2100, representing a staggering increase of 206.34%, whereas the EPA value declines from 11.34 million by 2030 to 8.05 million by 2100, indicating a decrease of 28.97%.

Fig. 4b shows that for all three scenarios, there is a discernible upward trend in the proportions of EGA in relation to the total GDP of CCZ as well as EPA relative to the entire population of CCZ from 2030 to 2100. Notably, under the RCP8.5-SSP5 scenario, the growth in the proportions of EGA and EPA is most pronounced: EGA jumps from 3.24% to 4.37%, while EPA surges from 3.88% to 5.09% over the 2030 to 2100 period. Conversely, under the RCP2.6-SSP1 scenario, the proportions of EGA and EPA experience the smallest growth, with EGA increasing from 3.25% to 3.63% and EPA rising from 3.61% to 4.02% within the same timeframe. In general, the GDP and population of the CCZ are projected to experience considerable repercussions due to coastal flooding, especially under the RCP8.5-SSP5 scenario.

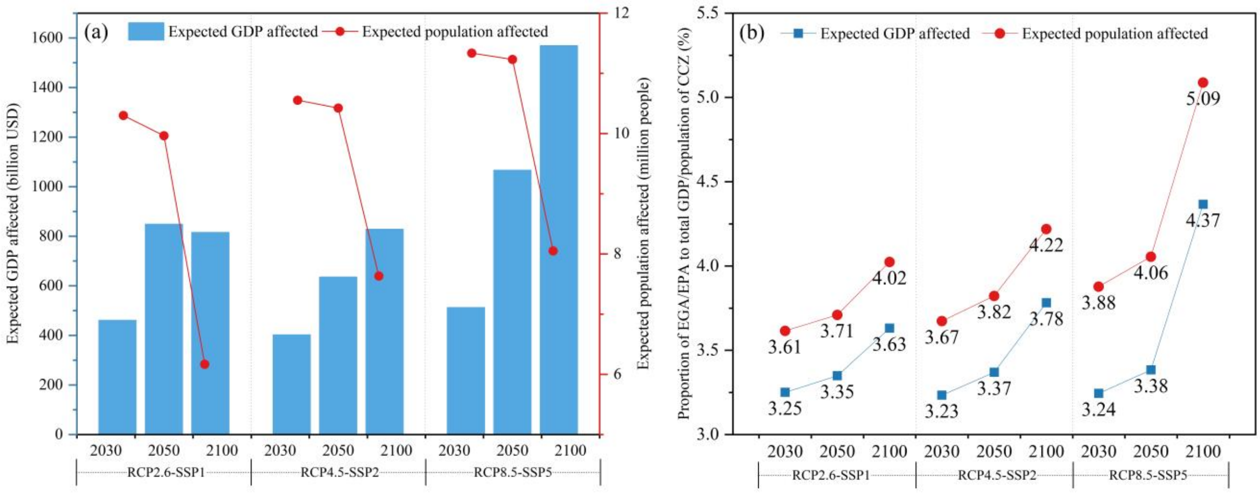

Fig. 4. Values (a) and proportion (b) of EGA and EPA in the CCZ under RCP2.6-SSP1, RCP4.5-SSP2, and RCP8.5-SSP5 by 2030, 2050, and 2100

By zooming to the coastal cities, Fig. 5 illustrates the spatiotemporal variation of EGA and EPA under the different scenarios over the pre-defined temporal scales in the coastal cities of the CCZ. The results indicate that there is significant spatial heterogeneity in the distribution of EGA and EPA within the coastal cities. Referring to the city IDs listed in Table S1 and shown in Fig. 5, it is evident that there are two identical distinct high-value agglomerations of EGAs and EPAs, cities numbered 46 to 52 that are primarily located in Guangdong and cities numbered 22 to 26 that are primarily located in Jiangsu. These coastal cities include Lianyungang (22), Yancheng (23), Nantong (24), Shanghai (25), Suzhou (26), Shenzhen (46), Dongguan (47), Guangzhou (48), Foshan (49), Zhongshan (50), and Jiangmen (52). In the entire China's coastal zone, coastal cities in Guangdong have the largest numbers of EGA and EPA values. For instance, Guangzhou (48) and Foshan (49) can be seen having much greater EGA and EPA values than other coastal cities. Particularly under the RCP8.5-SSP5 scenario, Guangzhou (48) experiences its peak for EGA of \$267.46 billion by 2100 and for EPA of 1953.96 thousand people by 2050, while Foshan (49) reaches peaks of \$260.75 billion in EGA and 1721.94 thousand people in EPA during the same time.

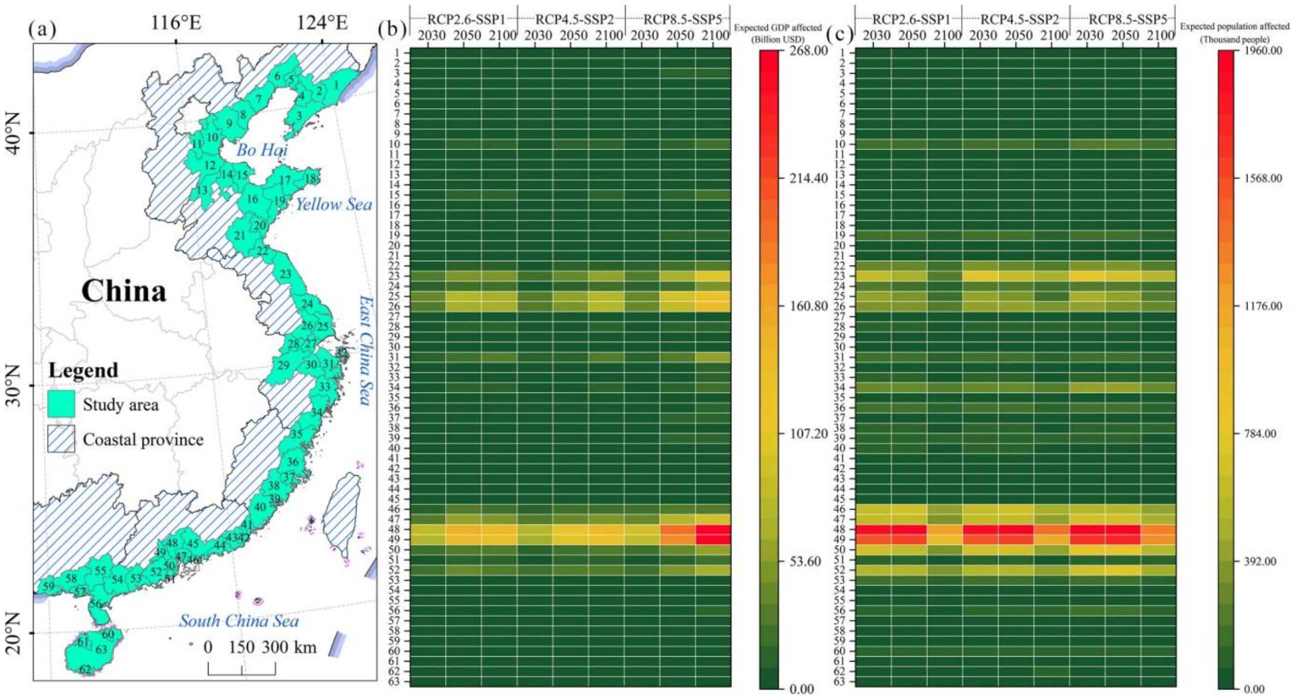

Fig. 5. EGA and EPA in different coastal cities of the CCZ by 2030, 2050, and 2100 under RCP2.6-SSP1, RCP4.5-SSP2, and RCP8.5-SSP5: (a) the coastal cities of CCZ; (b) EGA; and (c) EPA

3.2 Future socioeconomic development level assessment

3.2.1 Spatiotemporal dynamics of SDL in the CCZ

Fig. 6 indicates the spatiotemporal dynamics of the five levels of SDL under different future scenarios. Notably, the "Typical" level is dispersed in clusters and is predominantly located in the following coastal zones: central Liaoning, northern Hebei, central Tianjin, eastern Shandong, Shanghai, northeastern Zhejiang, and southeastern Guangdong. Furthermore, regions marked as "High" level are often observed near those designated as "Very high" level.

With regard to the area change, from 2030 to 2100, the area of "Typical" level displays an overall increasing trend under all three scenarios. For instance, under the RCP2.6-SSP1 scenario, this area increases from 10.98×10^3 km^2 by 2030 to 13.24×10^3 km^2 by 2050 and then decreases to 11.33×10^3 km^2 by 2100, with a change rate of 3.20% from 2030 to 2100; under the RCP4.5-SSP2 scenario, the area of the "Typical" level continuously expands from 11.23×10^3 km^2 by 2030 to 12.86×10^3 km^2 by 2100, with a change rate of 14.59% between 2030 and 2100; under the RCP8.5-SSP5, the "Typical" level area increases considerably from 12.74×10^3 km^2 by 2030 to 16.30×10^3 km^2 by 2050, and slightly shrinks to 15.82×10^3 km^2 by 2100, accounting for an overall 24.18% variation. Generally, SDL in the CCZ maintains a continuous rise under the RCP4.5-SSP2 scenario, fluctuates most significantly under the RCP8.5-SSP5 scenario despite the highest level of socioeconomic development up to 2100. Conversely, it consistently remains at its lowest under RCP2.6-SSP1 up to 2100.

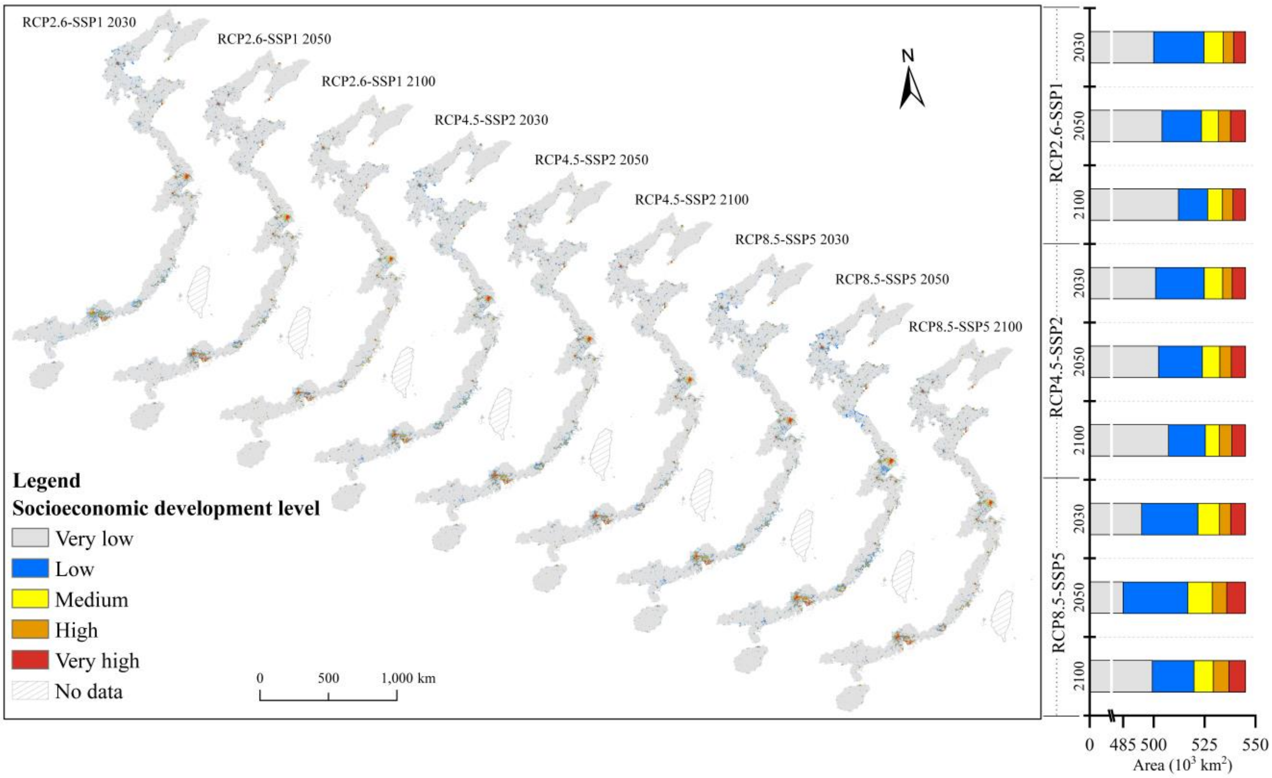

Fig. 6. Spatiotemporal distribution of SDL by 2030, 2050, and 2100 under RCP2.6-SSP1, RCP4.5-SSP2, and RCP8.5-SSP5 (side bars showing the total area in CCZ affected under different SDL levels)

3.2.2 Dynamics of mean SDL in coastal cities

To further explore the spatiotemporal dynamics of the SDL in coastal cities under various scenarios, Fig. 7 presents the distribution and quantitative characteristics of coastal cities in terms of MSDL. Cities such as Shenzhen (46) and Dongguan (47) in the Pearl River Delta region predominantly exhibit a “Very High” MSDL. And cities such as Xiamen (39), Shantou (42), Shanghai (25), Jiaxing (27), Guangzhou (48) and Foshan (49) mainly fall at the “High” level category. The “Medium” level coastal cities are dispersed across Tangshan (9), Tianjin (10), Langfang (11) in the western Bohai Sea, Qingdao (19) in the northern Jiaozhou Bay, Ningbo (31) in the southern Hangzhou Bay, Putian (37) in the Fujian coastal zone and Quanzhou (38), and Chaozhou (41), Jieyang (43), and Zhuhai (51) in the Guangdong coastal zone. There is a significant number of “Very low” and “Low” level cities, displaying a distinct north-south alternating spatial pattern. Notably, Suzhou (26) ascends from the “Medium” to the “High” and then descends to the “Medium” level in the RCP2.6-SSP1 scenario. In the two other scenarios, Suzhou (26) advances from the “Medium” level in 2030 to the

"High" level in 2050 and remains at that level beyond. Moreover, Zhongshan (50) falls from "High" level in 2050 down to "Medium" level by 2100 in the RCP2.6-SSP1 scenario but remains at "High" level under the rest of the scenarios.

From 2030 to 2100, variations in the number of cities across different MSDL levels are evident under various scenarios, with the exception of Shenzhen and Dongguan, which consistently maintain a "Very High" level. Under the RCP2.6-SSP1 scenario, there's a marked shift in cities at the "Very Low" and "Low" levels, with an increase of 5 cities in the former and a decrease of 4 in the latter. Cities categorized under "Medium" and "High" levels display a trend of initial increase followed by a decrease, resulting in an overall reduction by 0 and 1 cities, respectively. Under the RCP4.5-SSP2 scenario, there is an increase of 1 city each in the "Very Low", "Medium", and "High" levels, while cities at the "Low" level decrease by 3. As for the RCP8.5-SSP5 scenario, the "Very Low" level shows a significant decrease by 3 cities. In contrast, the "Low" and "High" levels experience a modest increase, by 2 and 1 cities respectively. The "Medium" level cities initially increase and then decrease, resulting in 0 net change.

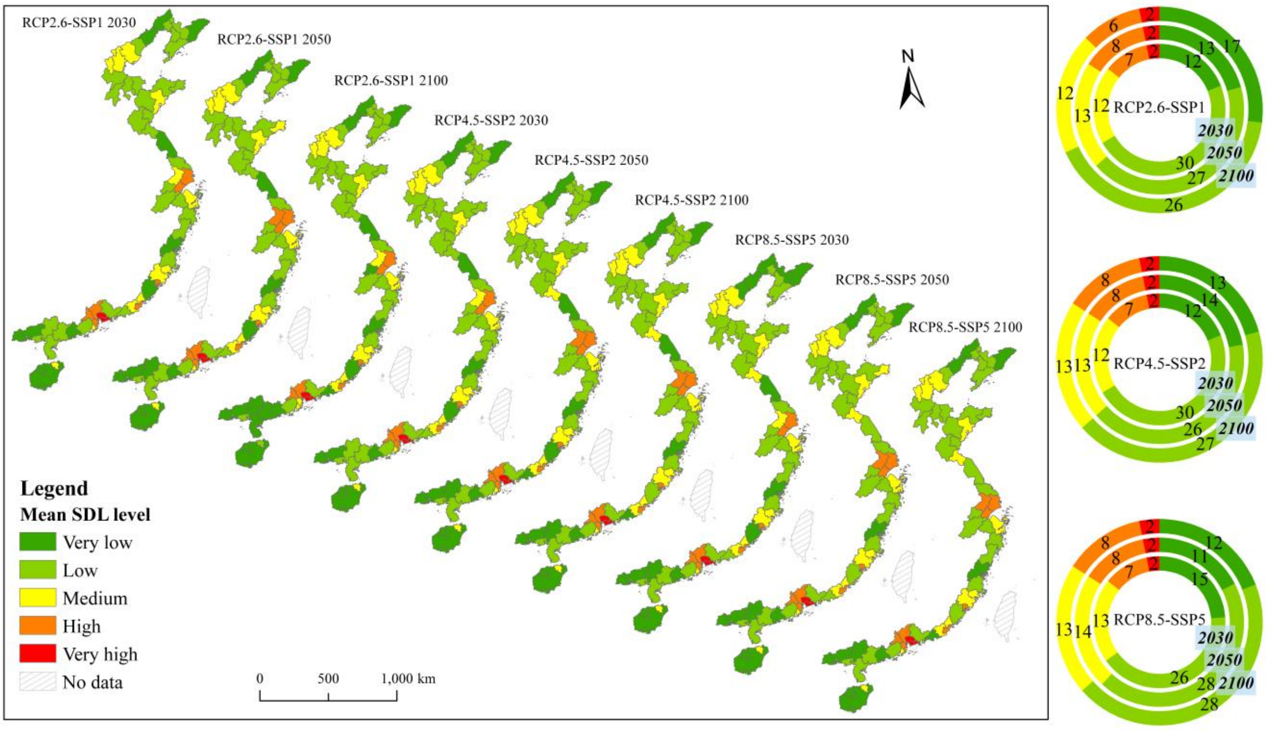

Fig. 7. MSDL level in different coastal cities in CCZ by 2030, 2050, and 2100 under RCP2.6-SSP1, RCP4.5-SSP2, and RCP8.5-SSP5 (side bars showing the number of coastal cities in CCZ under different MSDL levels)

3.3 Coupling coordination degree analysis

3.3.1 Spatiotemporal dynamics of CCD in the CCZ

Fig. 8 depicts the spatiotemporal distribution of CCD between CFR and SDL. The results indicate that the spatiotemporal patterns of CCD are rather similar across various scenarios over all periods at the macro-scale. The “Typical” level and “Medium” level are clustered in block-shaped distributions, while the “Low” level is dispersed, and the “Very low” level has a broad distribution without a definitive patter. Notably, the “Typical” and “Medium” levels are prominent along the coastal regions of Tianjin, northern Jiangsu, Shanghai, northern Zhejiang, eastern and southern Fujian, and the central part of Guangdong. The “Low” level, however, mainly prevails in the middle of Liaoning’s coast, extending from the Hebei coast toward the northern region of Zhejiang’s coast, the eastern coast of Guangxi, and the eastern coast of Hainan.

From 2030 to 2100, the spatial dynamics of the five CCD levels exhibit notable variances under different scenarios. The levels, ordered by area from largest to smallest, are as follows: “Very Low”, “Medium”, “Low”, and “Typical”. Notably, the “Typical” level, despite covering the smallest area, plays a crucial role in demonstrating the interrelation between CFR and SDL. Under the RCP2.6-SSP1 and RCP4.5-SSP2 scenarios, the area of “Typical” level demonstrates a fluctuating downward trend, contrasting with an overall increasing trend under the RCP8.5-SSP5 scenario. For instance, under the RCP2.6-SSP1 scenario, the area of the “Typical” level slightly increase from 24.64×10^3 km^2 by 2030 to 25.31×10^3 km^2 by 2050, and then sharply decreased to 20.84×10^3 km^2 by 2100, amounting to a total reduction of 15.44%; Under the RCP4.5-SSP2 scenario, it slightly increases from 25.09×10^3 km^2 by 2030 to 25.70×10^3 km^2 by 2050 and then decreases significantly to 23.56×10^3 km^2 by 2100, with an overall decrease of 6.12%; Under the RCP8.5-SSP5 scenario, the area experiences a drastic growth from 27.97×10^3 km^2 by 2030 to 31.60×10^3 km^2 by 2050, followed by a gradual decline to 28.77×10^3 km^2 by 2100, resulting in an overall increase of 2.87%. Additionally, the area of “Medium” level remains relatively stable under the RCP2.6-SSP1 scenario but shows a significant upward trend under the other two scenarios. Specifically, under the RCP2.6-SSP1 scenario, the area of “Medium” level slightly decreases from 55.83×10^3 km^2 by 2030 to 55.81×10^3 km^2 by 2100. Conversely, under the RCP4.5-SSP2 and RCP8.5-SSP5 scenarios, the area of “Medium” level consistently expands, growing from 57.93×10^3 km^2 to 62.37×10^3 km^2 and from 61.25×10^3 km^2 to 70.54×10^3 km^2 by 2100, respectively, with growth rates of 7.66% and 15.17%.

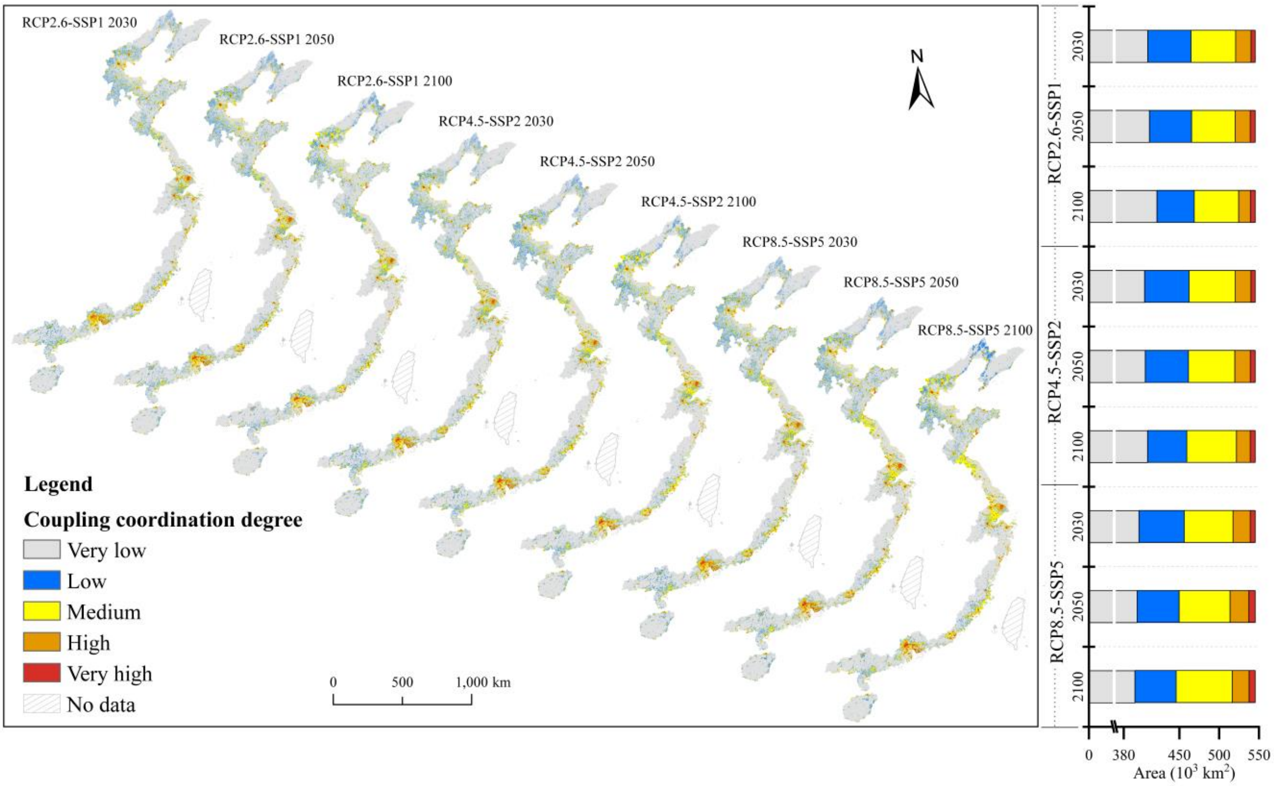

Fig. 8. Spatiotemporal distribution of CCD in CCZ by 2030, 2050, and 2100 under RCP2.6-SSP1, RCP4.5-SSP2, and RCP8.5-SSP5 (bars showing the total area in CCZ affected under different CCD level)

3.3.2 Dynamics of mean CCD in coastal cities

To further explore the spatiotemporal dynamics of the CCD in coastal cities under various scenarios, Fig. 9 shows the MCCD levels of the coastal cities in CCZ. The results indicate that the spatiotemporal variation patterns of the MCCD levels are largely harmonized across the scenarios at the macro-scale. From 2030 to 2100, the cities at "Typical" MCCD levels are primarily situated along the northern coast of Jiangsu, Zhejiang, and Shanghai, as well as the Pearl River Delta region. This encompasses a collective of 11 coastal cities: Lianyungang (22), Shanghai (25), Suzhou (26), Jiaxing (27), Xiamen (39), Shantou (42), Shenzhen (46), Dongguan (47), Guangzhou (48), Foshan (49), and Zhongshan (50). Cities maintaining a consistent "Medium" level are chiefly located in the coastal zones of Hebei, Shandong, Zhejiang, Fujian, Guangxi, and Hainan, enveloping 12 coastal cities: Cangzhou (12), Binzhou (14), Dongying (15), Weihai (18), Qingdao (19), Ningbo (31), Zhoushan (32), Putian (37), Quanzhou (38), Chaozhou (41), Beihai (57), and Haikou (60). Meanwhile, the number of cities at "Low" and "Very low" MCCD levels is more substantial, with a wider distribution, dominantly found along the coastlines of Liaoning, Shandong, Zhejiang, Fujian, Guangxi, and Hainan. Conclusively, the CCD is more salient in central and southern sectors of the CCZ, notably in the Yangtze River Delta and the Pearl River Delta.

Coastal cities classified at the "Typical" MCCD level are in need of extra attention to the interplay between socioeconomic development and coastal flood risk. Between 2030 and 2100, the number of cities at the “Typical” level fluctuates considerably across different scenarios. For example, under the RCP2.6-SSP1 scenario, a gradual decline is observed, with numbers reducing from 15 by 2030 to 13 by 2100. In contrast, under the RCP4.5-SSP2 scenario, the number remains consistent at 13 throughout the period. However, under the RCP8.5-SSP5 scenario, the number initially decreases from 15 by 2030 to 11 by 2050, then slightly rises to 12 by 2100. It is worth noting that under the higher emissions scenario, the number of cities in the "Very high" level accounts for a larger proportion of the number of cities in the “Typical” level by 2100. Specifically, by 2030, under all three scenarios, there are 6 cities at the “Very High” level, including Jiaxing (27), Shantou (42), Shenzhen (46), Dongguan (47), Foshan (49), and Zhongshan (50). By 2050, under the RCP2.6-SSP1 and RCP4.5-SSP2 scenarios, the number of cities at the same level remains unchanged. However, under the RCP8.5-SSP5 scenario, there is a notable reduction, with Shantou (42), Foshan (49), and Zhongshan (50) dropping to the “High” level. By 2100, there are significant changes in the number of cities at this level under all three scenarios. Under the RCP2.6-SSP1 scenario, there is the largest decrease, with only Shenzhen (46) and Dongguan (47) remaining at this level. Under the RCP4.5-SSP2 scenario, the number is also reduced by half, leaving Jiaxing (27), Shenzhen (46), and Dongguan (47) at this level. Conversely, under the RCP8.5-SSP5 scenario, an escalation is observed, with Lianyungang and Foshan ascending from the "High" to "Very High" level, while Jiaxing, Shenzhen, and Dongguan maintain their status at the "Very High" level.

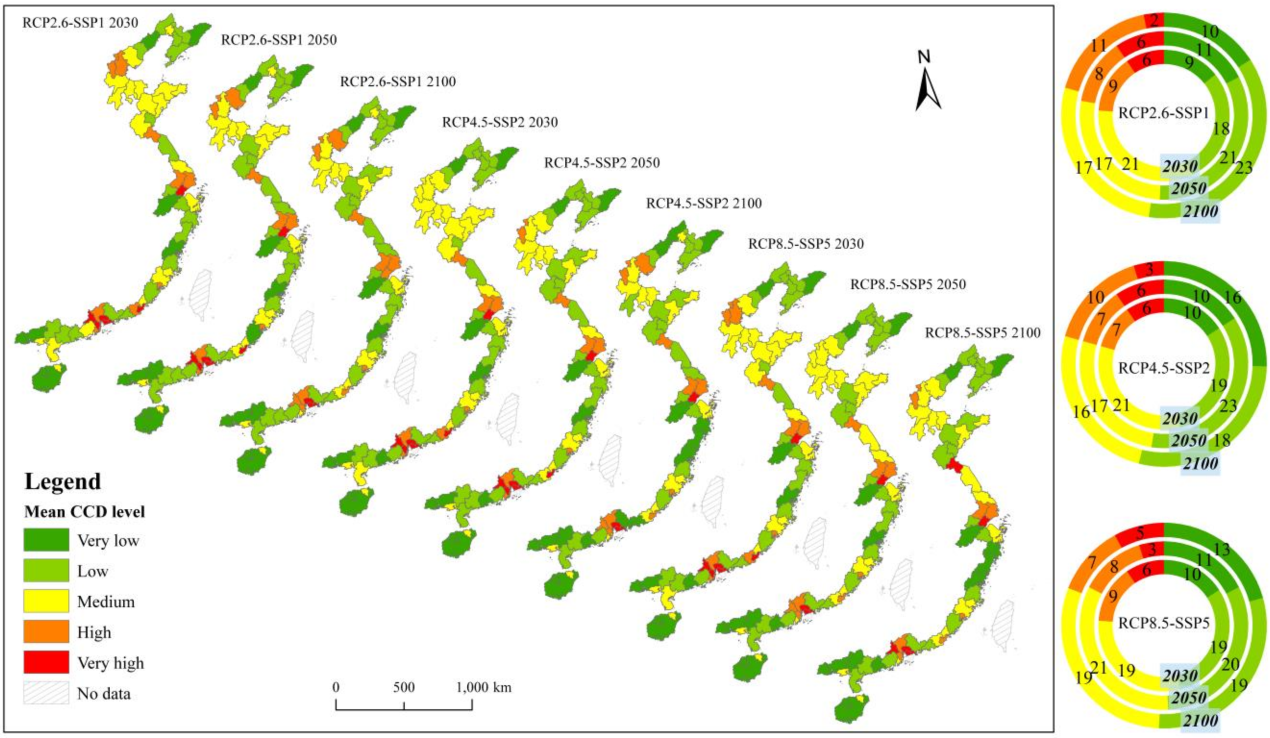

Fig. 9. MCCD level in different coastal cities of the CCZ by 2030, 2050, and 2100 under RCP2.6-SSP1, RCP4.5-SSP2, and RCP8.5-SSP5, respectively. (side bars showing the numbers of coastal cities in CCZ under different MCCD levels)

4. Discussion

In this study, we identified and quantified the spatiotemporal variation and quantitative characteristics of expected GDP and population affected by coastal flooding in the future period under three scenarios, assessed and demonstrated the characteristics of spatiotemporal variations in the socioeconomic development level of the CCZ, as well as analyzing the coupling coordination degree between the socioeconomic development level and coastal flood risk. The findings of this study are of great significance for enhancing CFR understanding and management at the national scale.

4.1 Expected socioeconomic impact of coastal flooding

Regarding the expected socioeconomic impact of coastal flooding, it is observed that the proportions of EGA and EPA in the total GDP and population of CCZ are on an increasing trend from 2050 to 2100, despite their individual trends of rise and fall, respectively (Fig. 4a and 4b). The decrease in EPA is likely due to the projected decline in CCZ's total population. Relevant studies suggest that during this period, the inundation area of CCZ is expected to increase by 2.71×10^3 km^2, 4.14×10^3 km^2, and 6.98×10^3 km^2 under the RCP2.6, 4.5, and 8.5 scenarios, respectively (Xu et al., 2022b). Simultaneously, the population in China's coastal provinces (excluding Hong Kong, Macau, and Taiwan) is expected to decrease by 245.22 million, 185.73 million, and 251.37 million under the SSP1, SSP2, and SSP5 scenarios, respectively (Chen et al., 2020). The increasing proportions of EGA and EPA, especially in pivotal provinces such as Jiangsu and Guangdong, suggest that if additional adaptation strategies are not developed, coastal flooding could adversely affect the stability and growth of China's overall economy. For instance, the increase in the EGA's share could lead to a loss of economic resources and a slowdown in growth rate. Similarly, the escalation in EPA's share could trigger more frequent population migrations in coastal areas, exerting extra pressure on the public services and housing markets of inland cities. Consequently, the government may need to bolster fiscal spending to manage disasters, and growing insurance costs could further burden businesses and residents financially. Furthermore, given the vital role of CCZ in global trade (Du et al., 2022), any serious infrastructural damage could severely disrupt international supply chains. Escalating disaster risks also threaten to worsen environmental degradation and social instability. In response, the Chinese government has formulated several policies at the national level to mitigate the socioeconomic impact of coastal flooding, achieving certain results. For example, in recent years, China has carried out the "Southern Mangrove and Northern Tamarisk" wetland restoration project (State Council of the P. R. China, 2016), launched the first national natural disaster risk survey (State Council of the P. R. China, 2020), established "carbon peak and neutrality" targets (The Communist Party of China Central Committee and the State Council of the P. R. China, 2021), formulated the series of standards for coastal zone protection and rehabilitation projects (Ministry of Natural

Resources of the P. R. China, 2022), issued the “National climate change adaptation strategy 2035”(Ministry of Ecology and Environment of the P. R. China, 2022) and the “National comprehensive disaster prevention and Mitigation Plan for the 14th Five-Year Plan” (Ministry of Emergency Management of the P. R. China, 2022). However, in the face of the conflict between increasing CFR and SDL, policymakers need to further integrate environmental, economic, and social stability considerations in future specific adaptation and mitigation strategies at the provincial and urban scale.

4.2 Prospective socioeconomic development and potential threats

By assessing the future socioeconomic development level of the CCZ, the findings highlight the crucial role of the Pearl River Delta (PRD), Yangtze River Delta (YaRD), and Tianjin-Hebei (TH) agglomerations in driving the future socioeconomic development of the CCZ, exhibiting the highest level of socioeconomic development (Fig. 6 and 7). The PRD, noted for its advanced manufacturing, Internet-based companies, and innovative Special Economic Zone policies, has risen as one of pivotal hubs of global innovation, with a significant impact on globalization and international trade (Chan et al., 2021). Nevertheless, this region faces significant risks from coastal flooding due to SLR, intense storm surges, low elevation, and dense riverine networks. Without effective adaptation policies, such risks could undermine the export-oriented manufacturing sectors and impede critical technological development, threatening regional economic stability and global technological progress (Chen et al., 2021). Similarly, the YaRD, centered around Shanghai and incorporating economically prosperous cities such as Suzhou and Hangzhou, forms a formidable economic hub. This region persistently draws in innovative sectors including new energy vehicles, fintech, and biomedicine, playing a pivotal role in linking China with the global economic network. However, it is also vulnerable to coastal flooding, with potential damage to its financial institutions, manufacturing facilities and major urban infrastructure (Lv et al., 2021). The TH urban agglomeration, as a part of Beijing-Tianjin-Hebei region, occupies a strategic geographic position in northern China. The region has clear advantages in areas such as aerospace, renewable energy, and chemicals. Moreover, the port of Tianjin plays an important role in international trade and is an important gateway for North China to integrate into the global economy. However, coastal flooding poses significant risks to port facilities and logistics networks, which could have far-reaching impacts on regional and international trade networks. Additionally, there is an increased risk of severe damage to urban infrastructure (including roads, bridges, and residential areas) and factory plants due to surface subsidence superimposed on SLR (Li et al., 2020; Fang et al., 2022). In summary, while the PRD, YaRD, and TH agglomerations are crucial for China’s future socioeconomic development and play key roles in global trade, their vulnerabilities to coastal flooding and other environmental risks necessitate effective strategic responses to safeguard their continued growth and contributions to the global economy.

4.3 Insights into coastal flood adaptation strategies: A coupling analysis perspective

At the macro-scale, understanding the dynamic relationship between SDL and CFR under various future scenarios in CCZ is essential for effective resource allocation and priority setting by policymakers, particularly in areas where balancing economic growth with disaster risk reduction is crucial. Socioeconomic development can offer technical and financial support for solving flood inundation challenges, while effective flood control can foster an environment conducive to the sustainable growth of both the economy and society. Conversely, socioeconomic development leading to the expansion of construction land reduces surface runoff infiltration. Combined with high concentrations of population and economy, floods can easily cause substantial socioeconomic losses, limiting further development of the economy and society. Therefore, when formulating policies in CCZ, the government needs more comprehensive and complex strategies to address both flood risk and economic development needs, fully considering the interaction between the two, seeking benefits and avoiding harms, and pursuing a path of sustainable development.

Addressing the conflict between SDL and CFR is a challenging issue faced by regions with high CCDs. Notably, over 17% of the 63 coastal cities in China are classified as “Very high” or “High” MCCD levels under different scenarios and timeframes (Fig. 9). Specially, under the RCP8.5-SSP5 scenario, five cities (Lianyungang, Jiaxing, Shenzhen, Dongguan, and Foshan) are projected to remain at the “Very high” MCCD level by 2100, with Jiaxing, Shenzhen, and Dongguan maintaining this level from 2030 to 2100. Despite variations in their socioeconomic development levels during the same period, these cities exhibit close connections between SDL and CFR. In these regions, measures should be taken in terms of both advance planning to avoid risks and enhanced adaptation to reduce risks. The former could reduce the link between SDL and CFR from different perspectives by avoiding the placement of high-value key sectors and vulnerable population concentrations in areas that could be deeply affected by future coastal flooding when formulating urban planning on the basis of scientific projections of future SLR and flood inundation characteristics, as well as by restoring coastal wetlands, constructing green seawalls, and enhancing the capacity to withstand coastal flooding (Magnan et al., 2022). The latter involves building high-standard sponge cities, efficient urban drainage systems, comprehensive flood warning systems, planning evacuation routes, increasing emergency shelters, raising public disaster awareness, and improving catastrophe insurance system. Additionally, under the RCP4.5-SSP2 scenario, the highest growth rate (60%) is observed in the number of cities classified as “Very low” MCCD level from 2030 to 2100, accompanied by a notable decline (-50%) in the number of cities classified as “Very high” level, followed by the RCP2.6-SSP1 scenario. In these regions with low coupling coordination degree, it indicates that socioeconomic development has a lower impact on flood risk, and vice versa. Thus, the government could focus resources on solving major problems without overly worrying about the mutual influence between the two. Overall, from the perspective of coupled analysis, the government should choose a development pathway that is socioeconomically developed and with controllable coastal flood risk. This approach involves not only take comprehensive measures to strengthen investment in disaster prevention and mitigation in developed cities such as Shenzhen, Shanghai, and Tianjin, but also pay attention to the risk management in moderately developed or underdeveloped cities such as Lianyungang, Tangshan, and Langfang, so as to realize the sustainable development of the CCZ, and to help the realization of Sustainable Development Goals (SDGs).

4.4 Limitations and further research

Like most studies, this study also has certain uncertainties and limitations that warrant attention in subsequent studies. First, although the projected data used in this study, such as inundation depth, coastal flood risk, and socioeconomic projection data, are of superior quality and resolution than those commonly used, they unavoidably carry their inherent uncertainties that may affect the results. Second, in assessing future socioeconomic development levels, this study relied on three key indicators—population, GDP, and LULC—due to a lack of available prediction data, which may not encompass the complete range of influences on SDL in the CCZ. Third, it is worth noting the absence of validation analysis given that future events are unknown and can only be inferred based on known rules (Liu and Chen, 2021). Nonetheless, these limitations notwithstanding, our findings are of significant value in understanding the socioeconomic impacts of coastal flooding in the CCZ throughout the 21st century. This is mainly attributed to the comprehensive analysis carried out in this study, which not only examines the quantitative and spatial variations in the expected impacts of coastal flooding on population and GDP at the scale of the entire CCZ but also assesses the spatiotemporal variation of the CCD between SDL and CFR. Future research will concentrate on integrating depth-impact curves based on various types of land use/ land cover, enriching key socioeconomic indicators in the CCZ, and deepening our grasp on the ecological repercussions of coastal flooding.

5. Conclusions

In this study, we demonstrated the quantitative and spatiotemporal characteristics of the EGA/EPA due to coastal flooding in the future in the CCZ, evaluated the variation of the future SDL in the CCZ using the AHP-EW combined method, and analyzed the changing characteristics of the CCD between the CFR and SDL in the CCZ from 2030 to 2100. The results showed that by 2100, under the RCP2.6-SSP1, RCP4.5-SSP2, and RCP8.5-SSP5 scenarios, the number of EGA/EPA could potentially reach \$814.90 billion (6.17 million people), \$828.16 billion (7.63 million people), and \$1568.83 billion (8.05 million people), respectively; The proportions of EGA (EPA) relative to total GDP (population) of CCZ may increase to 3.63% (4.02%), 3.78% (4.22%), and 4.37% (5.09%), respectively. Coastal cities, particularly in Jiangsu and Guangdong provinces may grapple with heightened socioeconomic risks; The total area of the CCZ at the "Very high" and "High" SDL levels by 2100 could reach 11.33×10^3 km^2, 12.86×10^3 km^2, and 15.82×10^3 km^2, respectively. The Pearl River Delta, Yangtze River Delta, and Tianjin-Hebei urban agglomerations will continue as the engine for the CCZ's socioeconomic development in the future; The CCD's spatiotemporal characteristics over the CCZ are largely harmonized among scenarios. Specifically, cities include Lianyungang, Jiaxing, Shenzhen, Dongguan, and Foshan will need to balance SDL and CFR to attain sustainable development.

Acknowledgments

This work is supported by the Strategic Priority Research Program of the Chinese Academy of Sciences (XDA1906020) and the National Natural Science Foundation of China (No. 42176221).

References

Aitsi-Selmi, A., Murray, V., Wannous, C., Dickinson, C., Johnston, D., Kawasaki, A., Stevance, A.-S., Yeung, T., 2016. Reflections on a Science and Technology Agenda for 21st Century Disaster Risk Reduction. Int. J. Disaster Risk Sci. 7, 1-29. https://doi.org/10.1007/s13753-016-0081-x.

Chan, F.K.S., Yang, L.E., Scheffran, J., Mitchell, G., Adekola, O., Griffiths, J., Chen, Y., Li, G., Lu, X., Qi, Y., Li, L., Zheng, H., McDonald, A., 2021. Urban flood risks and emerging challenges in a Chinese delta: The case of the Pearl River Delta. Environ. Sci. Policy 122, 101-115. https://doi.org/10.1016/j.envsci.2021.04.009.

Chen, R., Zhang, Y., Xu, D., Liu, M., 2018. Climate Change and Coastal Megacities: Disaster Risk Assessment and Responses in Shanghai City, in: Mal, S., Singh, R.B., Huggel, C. (Eds.), Climate Change, Extreme Events and Disaster Risk Reduction: Towards Sustainable Development Goals. Springer International Publishing, Cham, pp. 203-216.

Chen, X., Zhang, H., Chen, W., Huang, G., 2021. Urbanization and climate change impacts on future flood risk in the Pearl River Delta under shared socioeconomic pathways. Sci. Total Environ. 762, 143144. https://doi.org/10.1016/j.scitotenv.2020.143144.

Chen, Y., Guo, F., Wang, J., Cai, W., Wang, C., Wang, K., 2020. Provincial and gridded population projection for China under shared socioeconomic pathways from 2010 to 2100. Sci. Data 7, 83. https://doi.org/10.1038/s41597-020-0421-y.

Cui, Q., Xie, W., Liu, Y., 2018. Effects of sea level rise on economic development and regional disparity in China. J. Clean Prod. 176, 1245-1253. https://doi.org/10.1016/j.jclepro.2017.11.165.

Deng, J., Che, T., Jiang, T., Dai, L., 2021. Suitability projection for Chinese ski areas under future natural and socioeconomic scenarios. Adv. Clim. Chang. Res. 12, 224-239. https://doi.org/10.1016/j.accre.2021.03.007.

Du, P., Hou, X., Xu, H., 2022. Dynamic Expansion of Urban Land in China's Coastal Zone since 2000. Remote Sens. 14. https://doi.org/10.3390/rs14040916.

Edmonds, D.A., Caldwell, R.L., Brondizio, E.S., Siani, S.M.O., 2020. Coastal flooding will disproportionately impact people on river deltas. Nat. Commun. 11, 4741. https://doi.org/10.1038/s41467-020-18531-4.

Engström, K., Olin, S., Rounsevell, M.D.A., Brogaard, S., Van Vuuren, D.P., Alexander, P., Murray-Rust, D., Arneth, A., 2016. Assessing uncertainties in global cropland futures using a conditional probabilistic modelling framework. Earth Syst. Dynam. 7, 893-915. https://doi.org/10.5194/esd-7-893-2016.

Fang, J., Lincke, D., Brown, S., Nicholls, R.J., Wolff, C., Merkens, J.L., Hinkel, J., Vafeidis, A.T., Shi, P., Liu, M., 2020. Coastal flood risks in China through the 21st century - An application of DIVA. Sci. Total Environ. 704, 135311. https://doi.org/10.1016/j.scitotenv.2019.135311.

Fang, J., Nicholls, R.J., Brown, S., Lincke, D., Hinkel, J., Vafeidis, A.T., Du, S., Zhao, Q., Liu, M., Shi, P., 2022. Benefits of subsidence control for coastal flooding in China. Nat. Commun. 13, 6946. https://doi.org/10.1038/s41467-022-34525-w.

Fang, Y., Yin, J., Wu, B., 2016. Flooding risk assessment of coastal tourist attractions affected by sea level rise and storm surge: a case study in Zhejiang Province, China. Nat. Hazards 84, 611-624. https://doi.org/10.1007/s11069-016-2444-4.

Gaffin, S.R., Rosenzweig, C., Xing, X., Yetman, G., 2004. Downscaling and Geo-spatial Gridding of Socio-economic Projections from the IPCC Special Report on Emissions Scenarios (SRES). Glob. Environ. Change-Human Policy Dimens. 14, 105-123. https://doi.org/10.1016/j.gloenvcha.2004.02.004.

Gan, L., Wang, Y., Wang, Y., Lev, B., Shen, W., Jiang, W., 2021. Coupling coordination analysis with data-driven technology for disaster–economy–ecology system: an empirical study in China. Nat. Hazards 107, 2123-2153. https://doi.org/10.1007/s11069-021-04787-6.

Gao, Z., Geddes, R.R., Ma, T., 2020. Direct and Indirect Economic Losses Using Typhoon-Flood Disaster Analysis: An Application to Guangdong Province, China. Sustainability 12. https://doi.org/10.3390/su12218980.

Hallegatte, S., Green, C., Nicholls, R.J., Corfee-Morlot, J., 2013. Future flood losses in major coastal cities. Nat. Clim. Chang. 3, 802-806. https://doi.org/10.1038/nclimate1979.

Hinkel, J., Lincke, D., Vafeidis, A.T., Perrette, M., Nicholls, R.J., Tol, R.S.J., Marzeion, B., Fettweis, X., Ionescu, C., Levermann, A., 2014. Coastal flood damage and adaptation costs under 21st century sea-level rise. Proc. Natl. Acad. Sci. U. S. A. 111, 3292-3297. https://doi.org/10.1073/pnas.1222469111.

Hu, L., Zhang, Q., Wang, G., Singh, V.P., Wu, W., Fan, K., Shen, Z., 2022. Flood disaster risk and socioeconomy in the Yellow River Basin, China. J. Hydrol.-Reg. Stud. 44, 101272. https://doi.org/10.1016/j.ejrh.2022.101272.

IPCC, 2019. IPCC Special Report on the Ocean and Cryosphere in a Changing Climate in: H.-O. Pörtner, D.C. Roberts, V. Masson-Delmotte, P. Zhai, M. Tignor, E. Poloczanska, K. Mintenbeck, A. Alegría, M. Nicolai, A. Okem, J. Petzold, B. Rama, N.M. Weyer (Eds.). Cambridge University Press, Cambridge, UK and New York, NY, USA.

IPCC, 2021. Climate Change 2021: The Physical Science Basis. Contribution of Working Group I to the Sixth Assessment Report of the Intergovernmental Panel on Climate Change, in: Masson-Delmotte, V., P. Zhai, A. Pirani, S. L. Connors, C. Péan, S.B., N. Caud, Y. Chen, L. Goldfarb, M. I. Gomis, M. Huang, K. Leitzell, E. Lonnoy, J. B. R. Matthews, T. K. Maycock, T. Waterfield, O. Yelekçi, R. Yu, B. Zhou (Eds.). Cambridge University Press, Cambridge, UK and New York, NY, USA.

Jiang, T., Su, B., Wang, Y., Huang, J., Jing, C., Gao, M., Wang, G., Lin, Q., Jiang, S., Liu, S., Luo, Y., 2022. Gridded datasets for population and economy under Shared Socioeconomic Pathways. https://doi.org/10.57760/sciencedb.01683.

Kirezci, E., Young, I.R., Ranasinghe, R., Lincke, D., Hinkel, J., 2023. Global-scale analysis of socioeconomic impacts of coastal flooding over the 21st century. Front. Mar. Sci. 9. https://doi.org/10.3389/fmars.2022.1024111.

Li, D., Hou, X., Song, Y., Zhang, Y., Wang, C., 2020. Ground subsidence analysis in Tianjin (China) based on Sentinel-1A data Using MT-InSAR Methods, Appl. Sci.-Basel, p. 5514.

Li, H., Xu, E., Zhang, H., 2021. Examining the coupling relationship between urbanization and natural disasters: A case study of the Pearl River Delta, China. Int. J. Disaster Risk Reduct. 55, 102057. https://doi.org/10.1016/j.ijdrr.2021.102057.

Liao, Q., Yu, G., Jiang, W., Lu, C., Ma, Y., Liu, K., Lin, Q., Wang, Y., 2019. Research on the Risk Assessment of Qingdao Marine Disaster Based on Flooding. Sustainability 11. https://doi.org/10.3390/su11020468.

Liu, C., Yang, M., Hou, Y., Xue, X., 2021. Ecosystem service multifunctionality assessment and coupling coordination analysis with land use and land cover change in China's coastal zones. Sci. Total Environ. 797, 149033. https://doi.org/10.1016/j.scitotenv.2021.149033.

Liu, Y., Chen, J., 2021. Future global socioeconomic risk to droughts based on estimates of hazard, exposure, and vulnerability in a changing climate. Sci. Total Environ. 751, 142159. https://doi.org/10.1016/j.scitotenv.2020.142159.

Liu, Y., Han, L., Pei, Z., Jiang, Y., 2023. Evolution of the coupling coordination between the marine economy and urban resilience of major coastal cities in China. Mar. Pol. 148, 105456. https://doi.org/10.1016/j.marpol.2022.105456.

Liu, Y., Huang, X., Yang, H., 2022. An integrated approach to investigate the coupling coordination between urbanization and flood disasters in China. J. Clean Prod. 375, 134191. https://doi.org/10.1016/j.jclepro.2022.134191.

Liu, Y., Wang, S., Wang, X., Jiang, D., Ravindranath, N.H., Rahman, A., Htwe Nyo, M., Vijitpan, T., 2020. Flood risk assessment in Bangladesh, India and Myanmar based on the AHP weight method and entropy weight method. Geogr. Res. 39, 1892-1906. https://doi.org/10.1016/j.gloenvcha.2004.02.004.

Lv, Y., Li, W., Wen, J., Xu, H., Du, S., 2021. Population pattern and exposure under sea level rise: Low elevation coastal zone in the Yangtze River Delta, 1990–2100. Clim. Risk Manag. 33, 100348. https://doi.org/10.1016/j.crm.2021.100348.

Magnan, A.K., Oppenheimer, M., Garschagen, M., Buchanan, M.K., Duvat, V.K.E., Forbes, D.L., Ford, J.D., Lambert, E., Petzold, J., Renaud, F.G., Sebesvari, Z., van de Wal, R.S.W., Hinkel, J., Pörtner, H.-O., 2022. Sea level rise risks and societal adaptation benefits in low-lying coastal areas. Sci Rep 12, 10677. https://doi.org/10.1038/s41598-022-14303-w.

Merkens, J.-L., Lincke, D., Hinkel, J., Brown, S., Vafeidis, A.T., 2018. Regionalisation of population growth projections in coastal exposure analysis. Clim. Change 151, 413-426. https://doi.org/10.1007/s10584-018-2334-8.

Merkens, J.-L., Reimann, L., Hinkel, J., Vafeidis, A.T., 2016. Gridded population projections for the coastal zone under the Shared Socioeconomic Pathways. Glob. Planet. Change 145, 57-66. https://doi.org/10.1016/j.gloplacha.2016.08.009.

Messner, F., 2007. Evaluating flood damages: guidance and recommendations on principles and methods, T09-06-01. Helmholz Unweltforschungszentrum (UFZ).

Ministry of Ecology and Environment of the P. R. China, 2022. National climate change adaptation strategy 2035. https://www.mee.gov.cn/xxgk2018/xxgk/xxgk03/202206/t20220613_985261.html (accessed 4 January 2024).

Ministry of Emergency Management of the P. R. China, 2022. National comprehensive disaster prevention and Mitigation Plan for the 14th Five-Year Plan. https://www.gov.cn/zhengce/zhengceku/2022-07/22/content_5702154.htm (accessed 4 January 2024).

Ministry of Natural Resources of the P. R. China, 2022. Series of standards for coastal zone protection and rehabilitation projects. http://www.hyjianzai.cn/article/jz_works/2/26831.html (accessed 4 January 2024).

Ministry of Natural Resources of the P. R. China, 2023. China's Sea Level Bulletin 2022. http://gi.mnr.gov.cn/202205/t20220507_2735509.html (accessed 4 January 2024).

Murakami, D., Yoshida, T., Yamagata, Y., 2021. Gridded GDP projections compatible with the five SSPs (Shared Socioeconomic Pathways). Front. Built Environ. 7. https://doi.org/10.3389/fbuil.2021.760306.

Nicholls, R.J., Cazenave, A., 2010. Sea-level rise and its impact on coastal zones. Science 328, 1517-1520. https://doi.org/10.1126/science.1185782.

Nicholls, R.J., Lincke, D., Hinkel, J., Brown, S., Vafeidis, A.T., Meyssignac, B., Hanson, S.E., Merkens, J.-L., Fang, J., 2021. A global analysis of subsidence, relative sea-level change and coastal flood exposure. Nat. Clim. Chang. 11, 338-342. https://doi.org/10.1038/s41558-021-00993-z.

O'Neill, B.C., Kriegler, E., Riahi, K., Ebi, K.L., Hallegatte, S., Carter, T.R., Mathur, R., van Vuuren, D.P., 2014. A new scenario framework for climate change research: the concept of shared socioeconomic pathways. Clim. Change 122, 387-400. https://doi.org/10.1007/s10584-013-0905-2.

Ramirez, R., Mukherjee, M., Vezzoli, S., Kramer, A.M., 2015. Scenarios as a scholarly methodology to produce "interesting research". Futures 71, 70-87. https://doi.org/10.1016/j.futures.2015.06.006.

Saaty, T.L., 2008. Decision making with the analytic hierarchy process. Int. J. Services. Sci. 1, 83-98. https://doi.org/10.1504/IJSSci.2008.01759.

Shi, X., Han, Z., Fang, J., Tan, J., Guo, Z., Sun, Z., 2020. Assessment and zonation of storm surge hazards in the coastal areas of China. Nat. Hazards 100, 39-48. https://doi.org/10.1007/s11069-019-03793-z.

Song, B., 2021. Multi-scenario simulation of LUCC in China's coastal zone based on SD-FLUS model Yantai Institute of Coastal Zone Research, Chinese Academy of Sciences. University of Chinese Academy of Sciences, Yantai, Shandong, PR. China.

Spirandelli, D.J., Anderson, T.R., Porro, R., Fletcher, C.H., 2016. Improving adaptation planning for future sea-level rise: understanding uncertainty and risks using a probability-based shoreline model. J. Plan. Educ. Res. 36, 290-303. https://doi.org/10.1177/0739456X16657160.

State Council of the P. R. China, 2016. The 13th Five-Year Plan for ecological and environmental protection. https://www.gov.cn/gongbao/content/2016/content_5148753.htm (accessed 4 January 2024).

State Council of the P. R. China, 2020. Notice on launching the first National Comprehensive Risk Survey of Natural disasters. https://www.gov.cn/zhengce/content/2020-06/08/content_5518034.htm (accessed 4 January 2024).
Sun, Y., Liu, S., Dong, Y., An, Y., Shi, F., Dong, S., Liu, G., 2019. Spatio-temporal evolution scenarios and the coupling analysis of ecosystem services with land use change in China. Sci. Total Environ. 681, 211-225. https://doi.org/10.1016/j.scitotenv.2019.05.136.
Tebaldi, C., Strauss, B.H., Zervas, C.E., 2012. Modelling sea level rise impacts on storm surges along US coasts. Environ. Res. Lett. 7, 014032. https://doi.org/10.1088/1748-9326/7/1/014032.
The Communist Party of China Central Committee and the State Council of the P. R. China, 2021. Working guidance for carbon dioxide peaking and carbon neutrality in full and faithful implementation of the new development philosophy. https://english.www.gov.cn/policies/latestreleases/202110/25/content_WS61760047c6d0df57f98e3c21.html (accessed 4 January 2024).
van Vuuren, D.P., Carter, T.R., 2014. Climate and socio-economic scenarios for climate change research and assessment: reconciling the new with the old. Clim. Change 122, 415-429. https://doi.org/10.1007/s10584-013-0974-2.
van Vuuren, D.P., Edmonds, J., Kainuma, M., Riahi, K., Thomson, A., Hibbard, K., Hurtt, G.C., Kram, T., Krey, V., Lamarque, J.-F., Masui, T., Meinshausen, M., Nakicenovic, N., Smith, S.J., Rose, S.K., 2011. The representative concentration pathways: an overview. Clim. Change 109, 5. https://doi.org/10.1007/s10584-011-0148-z.
Vousdoukas, M.I., Mentaschi, L., Voukouvalas, E., Bianchi, A., Dottori, F., Feyen, L., 2018. Climatic and socioeconomic controls of future coastal flood risk in Europe. Nat. Clim. Chang. 8, 776-780. https://doi.org/10.1038/s41558-018-0260-4.
Wang, T., Sun, F., 2022. Global gridded GDP data set consistent with the shared socioeconomic pathways. Sci. Data 9, 221. https://doi.org/10.1038/s41597-022-01300-x.
Wang, X., Hou, X., Wang, Y., 2017. Spatiotemporal variations and regional differences of extreme precipitation events in the Coastal area of China from 1961 to 2014. Atmos. Res. 197, 94-104. https://doi.org/10.1016/j.atmosres.2017.06.022.
Wu, Y., Zhong, P.-a., Xu, B., Zhu, F., Ma, B., 2017. Changing of flood risk due to climate and development in Huaihe River basin, China. Stoch. Environ. Res. Risk Assess. 31, 935-948. https://doi.org/10.1007/s00477-016-1262-2.
Xiao, K., Tamborski, J., Wang, X., Feng, X., Wang, S., Wang, Q., Lin, D., Li, H., 2022. A coupling methodology of the analytic hierarchy process and entropy weight theory for assessing coastal water quality. Environ. Sci. Pollut. Res. 29, 31217-31234. https://doi.org/10.1007/s11356-021-17247-2.
Xu, H., Hou, X., Li, D., Wang, X., Fan, C., Du, P., Song, B., 2022a. Spatial assessment of coastal flood risk due to sea level rise in China’s coastal zone through the 21st century. Front. Mar. Sci. 9. https://doi.org/10.3389/fmars.2022.945901.
Xu, H., Hou, X., Li, D., Zheng, X., Fan, C., 2022b. Projections of coastal flooding under different RCP scenarios over the 21st century: A case study of China's coastal zone. Estuar. Coast. Shelf Sci. 279, 108155. https://doi.org/10.1016/j.ecss.2022.108155.
Xu, L., He, Y., Huang, W., Cui, S., 2016. A multi-dimensional integrated approach to assess flood risks on a coastal city, induced by sea-level rise and storm tides. Environ. Res. Lett. 11,

014001. https://dx.doi.org/10.1088/1748-9326/11/1/014001.

Yan, B., Li, S., Wang, J., Ge, Z., Zhang, L., 2016. Socio-economic vulnerability of the megacity of Shanghai (China) to sea-level rise and associated storm surges. Reg Environ Change 16, 1443-1456. https://doi.org/10.1007/s10113-015-0878-y.

Yang, L., Scheffran, J., Qin, H., You, Q., 2015. Climate-related flood risks and urban responses in the Pearl River Delta, China. Reg Environ Change 15, 379-391. https://doi.org/10.1007/s10113-014-0651-7.

Abbreviations

AHP	analytic hierarchy process
CCD	coupling coordination degree
CCDM	coupling coordination degree model
CCZ	China’s coastal zone (CCZ)
CFR	coastal flood risk
CI	consistency index
CR	consistency ratio
EGA	expected GDP affected
EPA	expected population affected
EW	entropy weight
FVCOM	finite volume coastal and ocean model
GDP	gross domestic product
HCM	hydraulic connectivity model
IPCC	Intergovernmental Panel on Climate Change
LULC	land use/land cover
MSDL	mean of socioeconomic development level
MCCD	mean of coupling coordination degree
PAA	proportion of assets affected
RCP	representative concentration pathway
RI	random index
SD-FLUS	system dynamics-future land use simulation
SDGs	sustainable development goals
SDL	socioeconomic development level
SLR	sea level rise
SSP	shared socio-economic development pathway

Supplementary Material

Table S1 City information in China's coastal zone

City ID	City name	Area (km^2)	Province
1	Dandong	15290	Liaoning
2	Anshan	9255	Liaoning
3	Dalian	12574	Liaoning
4	Yingkou	5427	Liaoning
5	Panjin	4062	Liaoning
6	Jinzhou	10301	Liaoning
7	Huludao	10400	Liaoning
8	Qinhuangdao	7802	Hebei
9	Tangshan	13472	Hebei
10	Tianjin	11966	Tianjin
11	Langfang	6429	Hebei
12	Cangzhou	14304	Hebei
13	Dezhou	10356	Shandong
14	Binzhou	9660	Shandong
15	Dongying	8257	Shandong
16	Weifang	16185	Shandong
17	Yantai	13900	Shandong
18	Weihai	5800	Shandong
19	Qingdao	11293	Shandong
20	Rizhao	5375	Shandong
21	Linyi	17200	Shandong
22	Lianyungang	7615	Jiangsu
23	Yancheng	17700	Jiangsu
24	Nantong	8001	Jiangsu
25	Shanghai	6341	Shanghai
26	Suzhou	8657	Jiangsu
27	Jiaxing	3915	Zhejiang
28	Huzhou	5820	Zhejiang
29	Hangzhou	16850	Zhejiang
30	Shaoxing	8273	Zhejiang
31	Ningbo	9816	Zhejiang
32	Zhoushan	1400	Zhejiang
33	Taizhou	10050	Zhejiang
34	Wenzhou	12110	Zhejiang
35	Ningde	13452	Fujian
36	Fuzhou	11969	Fujian
37	Putian	4200	Fujian
38	Quanzhou	11015	Fujian
39	Xiamen	1701	Fujian
40	Zhangzhou	12600	Fujian

41	Chaozhou	3614	Guangdong
42	Shantou	2245	Guangdong
43	Jieyang	5269	Guangdong
44	Shanwei	4865	Guangdong
45	Huizhou	11347	Guangdong
46	Shenzhen	1997	Guangdong
47	Dongguan	2460	Guangdong
48	Guangzhou	7434	Guangdong
49	Foshan	3798	Guangdong
50	Zhongshan	1784	Guangdong
51	Zhuhai	1725	Guangdong
52	Jiangmen	9535	Guangdong
53	Yangjiang	7967	Guangdong
54	Maoming	11428	Guangdong
55	Yulin	12800	Guangxi
56	Zhanjiang	13263	Guangdong
57	Beihai	4018	Guangxi
58	Qinzhou	10897	Guangxi
59	Fangchenggang	6222	Guangxi
60	Haikou	2297	Hainan
61	Danzhou	3406	Hainan
62	Sanya	1921	Hainan
63	Other city in Hainan	27776	Hainan

Table S2 Scale of relative importance

Relative	Definition	Description
1	Equal importance	Two indicators influence on objective equally
3	Moderate importance	Experience and judgement slightly favor one indicator over another
5	Strong importance	Experience and judgement strongly favor one indicator over another
7	Very strong importance	One decision indicator is favored strongly over another and its supremacy
9	Extreme importance	The evidence favoring one decision indicator over another is of the highest
2, 4, 6, 8	Intermediate values between the two adjacent judgements	Compromise is needed

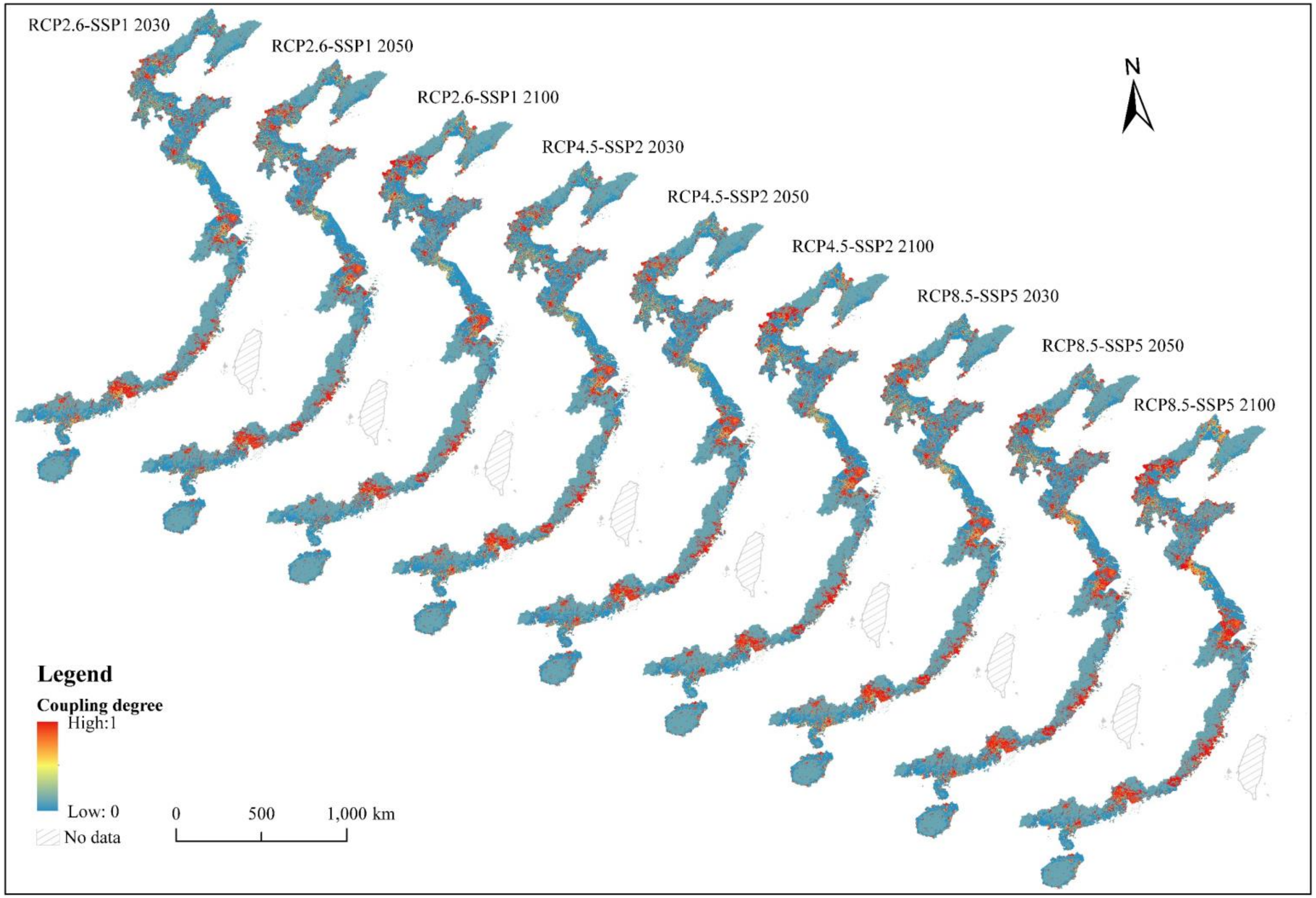

Fig. S1. Spatiotemporal distribution of coupling degree in the CCZ by 2030, 2050, and 2100 under RCP2.6-SSP1, RCP4.5-SSP2, and RCP8.5-SSP5, respectively.

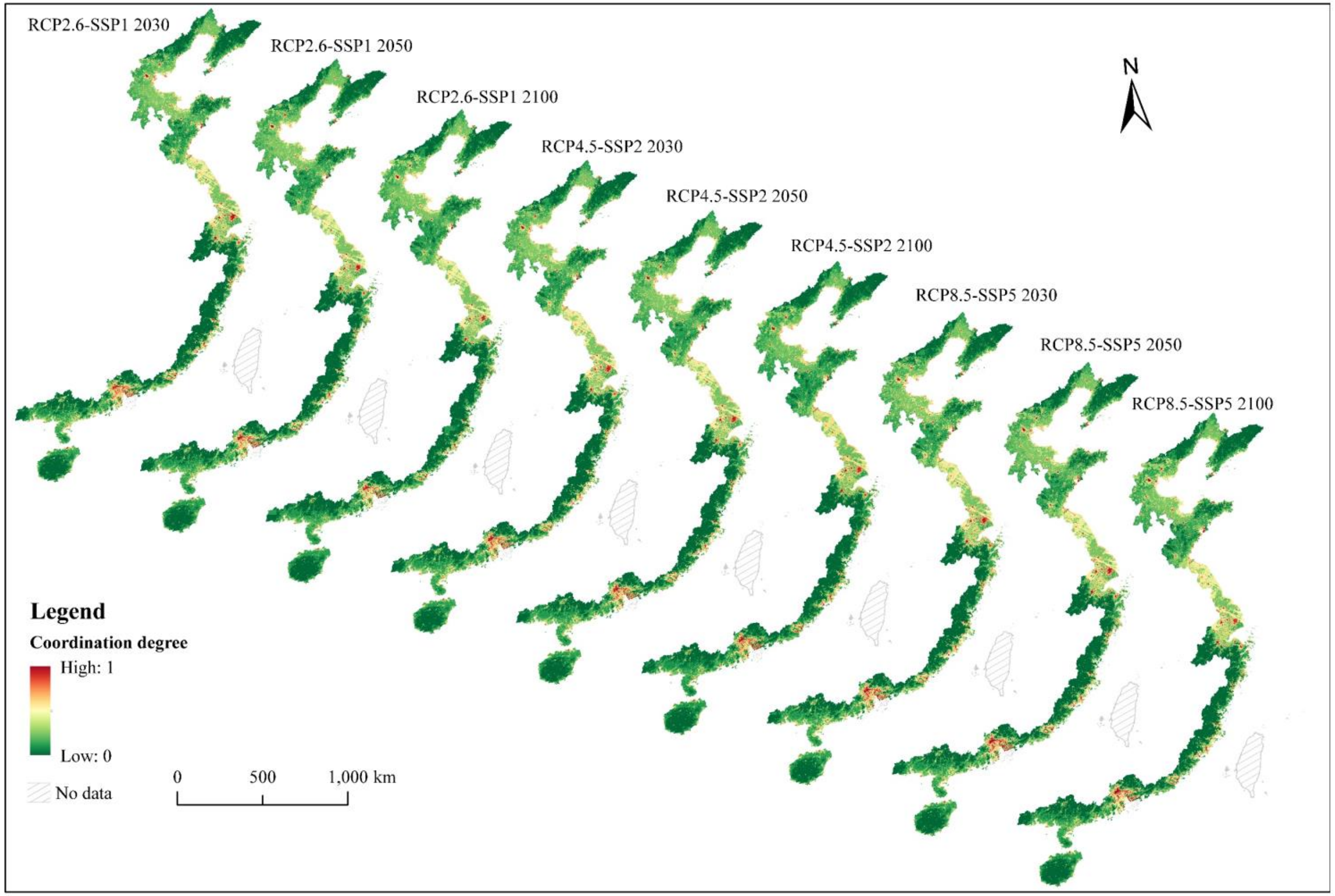

Fig. S2. Spatiotemporal distribution of coordination degree in the CCZ by 2030, 2050, and 2100 under RCP2.6-SSP1, RCP4.5-SSP2, and RCP8.5-SSP5, respectively.